Catena 247 (2024) 108470

Contents lists available at ScienceDirect

Catena

journal homepage: www.elsevier.com/locate/catena

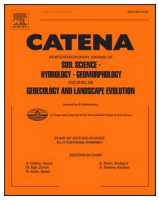

Clay composition heterogeneity in sediments from mountainous catchments with contrasting bedrock lithology in SE China coast

Ling Wang, Xing Jian *, Haowei Mei, Xiaotian Shen, Hanjing Fu

State Key Laboratory of Marine Environmental Science, College of Ocean and Earth Sciences, Xiamen University, Xiamen 361102, PR China

ARTICLE INFO

Keywords:
Clay mineral heterogeneity
Mountainous rivers
Source-to-sink processes
Zhe-Min rivers
SE China

ABSTRACT

Low-latitude mountainous rivers in South and East Asia play a crucial role in material cycles on the Earth's surface and are ideal targets to study how mountainous river sediments are generated, supplied and transported to continental margins. The Zhe-Min mountainous rivers in SE China coast are characterized by similar monsoon- and typhoon-induced high rainfall conditions to those islands in western Pacific (e.g., Taiwan) but have different geological backgrounds. With rather diverse bedrock types, intra- and inter-catchment differences of discharged sediment compositions of the Zhe-Min mountainous rivers remain poorly known. Here, we present clay mineral data of sediments from eight small–mesoscale mountainous rivers (drainage area < 80000 km^2 and maximum altitude > 1000 m) and two estuarine bays in this region to investigate spatial variations in sediment compositions and characterize supply, transport and deposition processes of the fine-grained sediments in these catchments. Significant spatial heterogeneity of clay minerals in the analyzed river sediments is observed, not only among these rivers, but also among non-tidal influenced reach, tidal reach and estuarine bay from the single river, implying complex accumulation process of the riverbed fine-grained sediments. Our quantitative analysis results reveal major controls of previously-underrated climate differences (e.g., temperature) and contrasting bedrock lithology on the clay mineral heterogeneity. The relatively low heterogeneity in clay mineral compositions between tidal reaches and bays, along with the widespread appearance of smectite in these regions, are distinctively different from those in the non-tidal influenced reaches. This reveals well-mixing of the offshore-sourced and mountain-supplied fine-grained sediments and highlights the major role of the tidal effects. This study demonstrates that determining terrigenous sediment output signals for small–mesoscale mountainous rivers with contrasting bedrock lithology and prevailing tidal water intrusion is a challenging job. Our findings have broad implications for chemical weathering intensity evaluation and sediment source-to-sink system studies.

1. Introduction

Rivers, as important passages connecting land (source) and oceans (sink), supply a large amount of fresh water, solutes, sediments, organic matter and pollutants to the oceans, which have significant impacts on biogeochemical cycles on the Earth's surface (Syvitski, 2003; Bianchi and Allison, 2009; Milliman and Farnsworth, 2013; Jian et al., 2020b). Large rivers (drainage area > 80000 km^2; Milliman and Farnsworth, 2013) have long been a focus of concern due to their great contributions of water and sediments to the global oceans (Milliman and Farnsworth, 2013; Ranasinghe et al., 2019). Large rivers generally develop wide alluvial plains where sediments may be recycled, redeposited and retransferred, showing complex sediment source-to-sink processes (Bi et al., 2015). In contrast, small–mesoscale mountainous rivers (drainage area < 80000 km^2 and maximum altitude > 1000 m; Milliman and Farnsworth, 2013) have insufficient accommodation to store sediments and are generally characterized by rapid sediment transport, exhibiting relatively simple sediment source-to-sink processes (Bao et al., 2015; Jian et al., 2020b). A growing number of researchers have realized that sediment fluxes of small–mesoscale mountainous rivers to the oceans are also significant despite their small basin areas (Milliman and Syvitski, 1992; Lyons et al., 2002; Kao and Milliman, 2008; Wheatcroft et al., 2010; Evrard et al., 2011; Milliman et al., 2017; Jian et al., 2020a). Sediments delivered by those small–mesoscale mountainous rivers are thought to exert significant impacts on landscapes, sedimentary environments and material cycles in estuary and coastal areas (Romans

* Corresponding author.
E-mail address: xjian@xmu.edu.cn (X. Jian).

https://doi.org/10.1016/j.catena.2024.108470
Received 9 January 2024; Received in revised form 29 August 2024; Accepted 13 October 2024
Available online 24 October 2024

et al., 2016; Jian et al., 2020b). Therefore, small–mesoscale mountainous exorheic rivers play a crucial role in the global land–ocean interface systems and have attracted considerable attention for decades (Milliman and Syvitski, 1992; Lyons et al., 2002; Farnsworth and Milliman, 2003; Coynel et al., 2005; Wheatcroft et al., 2010; Evrard et al., 2011; Yang and Yin, 2018; Sun et al., 2022).

Globally, low-latitude (< 30°) small–mesoscale mountainous rivers are particularly important sources and pathways of sediments to the coastal oceans (Milliman and Farnsworth, 2013; Jian et al., 2020b), for instance, the mountainous rivers developing in the South and East Asia regions. These rivers are under both tectonically-stable continent settings (e.g., SE China mainland, Fig. 1) and tectonically-active settings (e.g., Taiwan and Luzon, Fig. 1) (Bi et al., 2015; Jian et al., 2020a) and are affected by tropical or subtropical monsoon climate and typhoon weather with heavily seasonal precipitation. These conditions make the low-latitude South and East Asia ideal regions for studying how small–mesoscale mountainous river catchments generate, supply and transport sediments to continental margins. The Zhe-Min rivers along the SE China coast comprise several small–mesoscale mountainous rivers (Fig. 1B) and are previously considered as a third type of river system in subtropical East Asia (Jian et al., 2020a), in addition to those large rivers and tectonically-active island small mountainous rivers (drainage area < 10000 km^2). We realize that the Zhe-Min mountainous rivers have rather different bedrock types. However, intra- and inter-catchment differences in the discharged sediment compositions remain poorly known, hindering a deep understanding of the sediment source-to-sink system in this region.

Clay minerals are important products of rock chemical weathering on the Earth's surface and are widely distributed in soils and in river, lake and marine sediments (Mei et al., 2021; Warr, 2022; Lyu and Lu, 2024). Fine-grained sediments in rivers and oceans contain high proportions of clay minerals which is primarily originated from continental weathering processes (Fagel, 2007; Wu et al., 2022). Global distributions of clay minerals are thought to be mainly controlled by weathering process which is influenced by many factors (e.g., climate, bedrock lithology, topography, tectonic activities, etc.) (Ito and Wagai, 2017; Warr, 2022; Lyu and Lu, 2024). Therefore, clay mineralogy is an important means to study weathering processes on the Earth's surface and to reveal source-to-sink processes of river or marine sediments (Ehrmann et al., 2007; Fagel, 2007; Liu et al., 2016; Adriaens et al., 2018; Khan et al., 2019; Wang et al., 2023). Clay mineral compositions and related crystallochemical parameters (e.g., illite crystallinity) are widely applied to study sediment source-to-sink system and chemical weathering intensity of the small–mesoscale mountainous catchments in SE China (Liu et al., 2008, 2010, 2016; Xu et al., 2009; Li et al., 2012; Guo, 2014; Wang et al., 2016; Nayak et al., 2022). The rivers on the

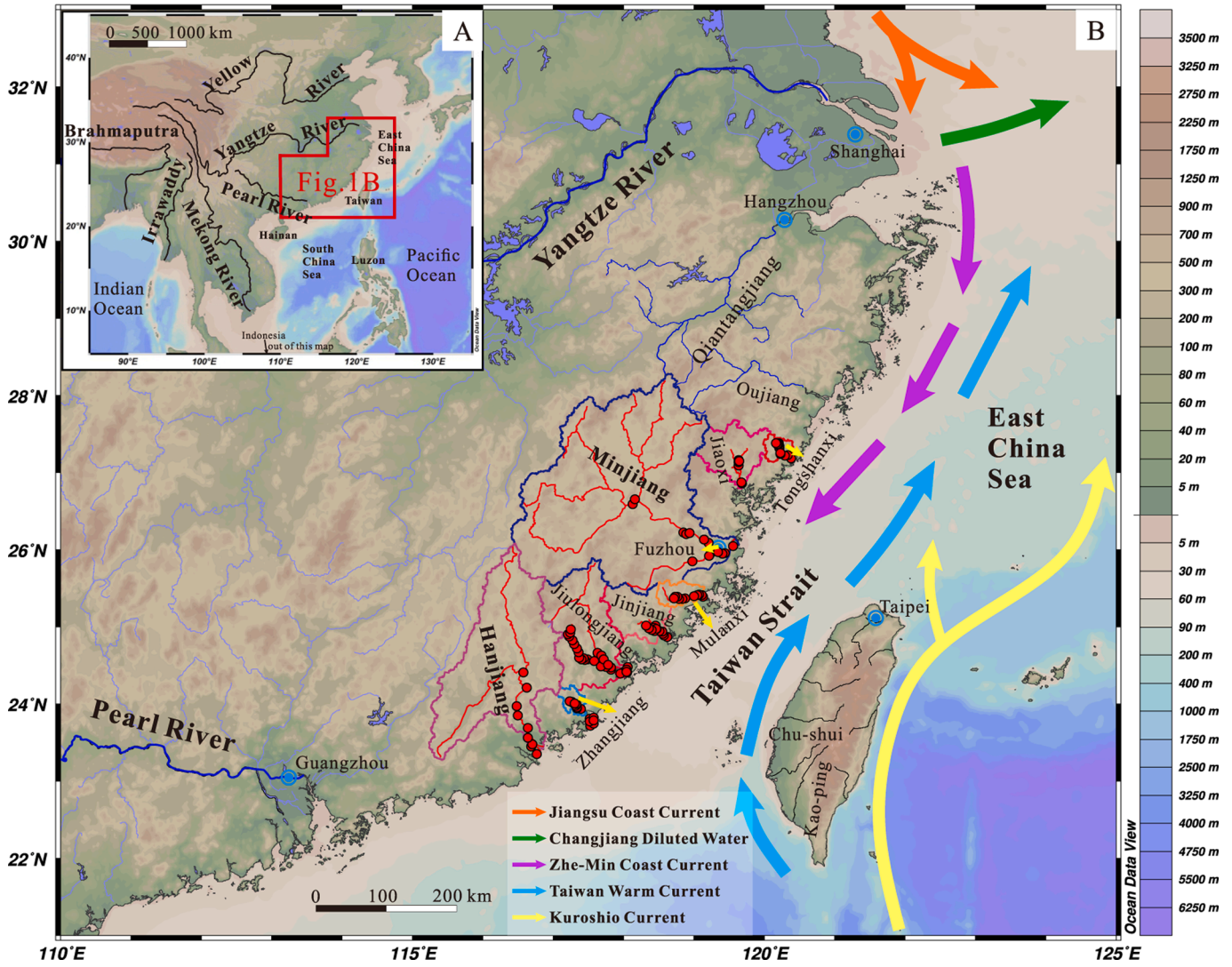

Fig. 1. (A) Large rivers in the East Asia margin. (B) Topography and drainage in subtropical Southeast China with sampling sites. Dominated currents in the Taiwan Strait and the East China Sea (ECS) are also shown.

tectonically-active islands (e.g., Taiwan) in this region have received great attention and clay mineralogical data therein have been widely reported. In these Taiwanese rivers, the predominant clay minerals are illite and chlorite (Liu et al., 2008, 2010, 2016; Li et al., 2012; Wang et al., 2016; Nayak et al., 2022; Zhang et al., 2022). However, clay mineralogical studies on sediments from the Zhe-Min mountainous rivers remain relatively insufficient. Limited investigation results (e.g., focusing on the Minjiang River and the Jiulongjiang River) (see Fig. 1B for locations) indicate that kaolinite is the main clay mineral species, formed primarily as a product of intense chemical weathering (Xu et al., 2009; Guo, 2014; Liu et al., 2016). However, data from the Mulanxi River (a very small mountainous river, see Fig. 1B for location) sediments indicate that illite is the predominant clay mineral (Guo, 2014). Despite the similar climatic background shared by small–mesoscale mountainous rivers in Taiwan and those in Zhe-Min regions, there are significant differences in the types of clay minerals. The clay minerals in sediments from the Taiwanese rivers are thought to be primarily influenced by intense tectonic activity, rapid erosion and properties of bedrock (Li et al., 2012; Liu et al., 2016). The controlling factors for clay minerals in the Zhe-Min rivers have yet to be clearly identified, although some studies have suggested that climate is an important controlling factor (e.g., He et al., 2020). We also note that these Zhe-Min mountainous rivers are influenced by strong tidal currents (Liu et al., 2021), but most sediment provenance studies on the East Asia continental margin tend to simply employ sediment signals from downstream or estuary regions as end-members for the river sources (e.g., Xu et al., 2009; Li et al., 2021b). How to determine clay mineralogical compositions of these small–mesoscale mountainous rivers as terrigenous output signatures when tracing marine sediment provenance is a challenging job. As tropical and subtropical mountainous rivers deliver a disproportionately large number of sediments to the global oceans (Milliman and Farnsworth, 2013), investigations on the clay mineral distributions in river sediments and unraveling related controls are important to better understand their source-to-sink processes and sediment cycles in the river-ocean systems.

To address these issues, we focus on eight small–mesoscale mountainous rivers and two estuarine bays in SE China coast (Fig. 1; Table 1). These river catchments have contrasting bedrock lithology (Table 1). Sediments were collected from riverbed and seafloor and clay minerals were then separated and analyzed. The aims are: to (1) investigate spatial variations in clay mineral compositions of these mountainous river sediments; to (2) unravel controlling factors of clay mineral distributions and to (3) decipher sediment source signals of small–mesoscale, tide-dominated, bedrock-contrasting, mountainous rivers using clay minerals.

2. Study area

Fluvial samples were collected from eight rivers in the SE China mainland coast, from north to south, including the Tongshanxi, Jiaoxi, Minjiang, Mulanxi, Jinjiang, Jiulongjiang, Zhangjiang and Hanjiang Rivers (Fig. 1B; Table 1). Seafloor surface sediment samples were collected from two related estuarine bays of the Jiulongjiang River and Zhangjiang River (also named as Xiamen Bay and Dongshan Bay in some literatures, respectively, Chen et al., 2021; Cui et al., 2022). All the studied rivers drain eastward across hilly or mountainous regions with maximum elevations of more than 1000 m (Table 1). These river basins are affected by a subtropical monsoon climate characterized by warm and humid conditions and frequent typhoon events (Su et al., 2017; Garzanti et al., 2021), with mean annual temperature (MAT) of 16–21 °C and mean annual precipitation (MAP) of 1300–1800 mm (Table 1).

All the river basins are developed on the tectonically-stable Cathaysia block. The SE part of the Cathaysia block is mainly composed of granite and volcanic rocks with ages younging eastward from Jurassic to Cretaceous (Fig. 2). The NW part of the Cathaysia block mainly comprises Precambrian metasedimentary rocks, Paleozoic

Table 1
Characteristics of the studied river catchments.

Rivers	Drainage Area (10^3 km^2)	Relief (m)	Mean basin slope (°)	MAT (°C)	MAP (mm/yr)	Water Discharge (10^8 m^3)	Sediment Load (10^4t/yr)	Tidal reach (km)	Main Lithology
Tongshanxi	0.425[a]	1141[a]	12.8	17.9[f]	1654[f]			~35[j]	93% clastic rocks
Jiaoxi	5.6[b]	1649[a]	15.3	16.5[f]	1790[f]	56.95 [g]	75.48[i]	~47[e]	79% clastic rocks + 19% granites
Minjiang	61[c]	2158[a]	14.2	18.3[f]	1687[f]	584.59 [g]	693.29[i]	~117 [k]	43% clastic rocks + 29% granites + 26% metamorphic rocks
Mulanxi	1.7[c]	1451[a]	11.0	20.1[f]	1301[f]	15.91 [g]	43.52[i]	26[l]	59% clastic rocks + 18% diorites + 12% granites
Jinjiang	5.6[b]	1600[a]	12.8	19.9[f]	1312[f]	51.44 [g]	257.23[i]	~20 [m]	65% clastic rocks + 27% granites
Jiulongjiang	14.7[c]	1823[a]	13.8	19.2[f]	1392[f]	147.62 [g]	369.95[i]	~20[n]	55% clastic rocks + 33% granites
Zhangjiang	1.038[d]	1117[e]	11.9	20.9[f]	1339[f]	11.09 [g]	41.9[d]	~13[o]	74% clastic rocks + 22% granites
Hanjiang	30.1[c]	1823[a]	11.4	20.3[f]	1518[f]	161.1 [h]		~10[p]	44% clastic rocks + 37% granites + 14% metamorphic rocks

[a] Data from Li et al. (2021a).
[b] Data from Li et al. (2019).
[c] Data from Garzanti et al. (2021).
[d] Data from Li et al. (2018).
[e] Data from Annals of Fujian Province [*Fujian Province Local Chronicles Compilation* Committee, 2001].
[f] Data from Peng (2019, 2020), representing average values for the entire basin and are calculated from averages of the range of 1981 to 2021. The datasets are provided by the National Tibetan Data Center (http://data.tpdc.ac.cn).
[g] Data from Fujian Province Water Resources Bulletin [Fujian Province Water Management Institute, 2021b].
[h] Data from Guangdong Province Water Resources Bulletin [Guangdong Province Water Management Institute, 2021].
[i] Data from Fujian Province Soil and Water Conservation Bulletin [Fujian Province Water Management Institute, 2021a].
[j] Data from Duanmu (2006).
[k] Data from Chen et al. (2023).
[l] Data from Li et al. (2021c).
[m] Data from Zhang et al. (2015).
[n] Data from Zhu (2001).
[o] Data from Zhang et al. (2012).
[p] Data from Shantou water resources information network (https://www.shantou.gov.cn/stwater).

The sediment load and water discharge are the sediment yield and water yield form river outlets to coastal seas. The mean basin slope was calculated by ArcGIS 10.8 based on 90-m resolution Digital Elevation Model (DEM) (https://srtm.csi.cgiar.org).

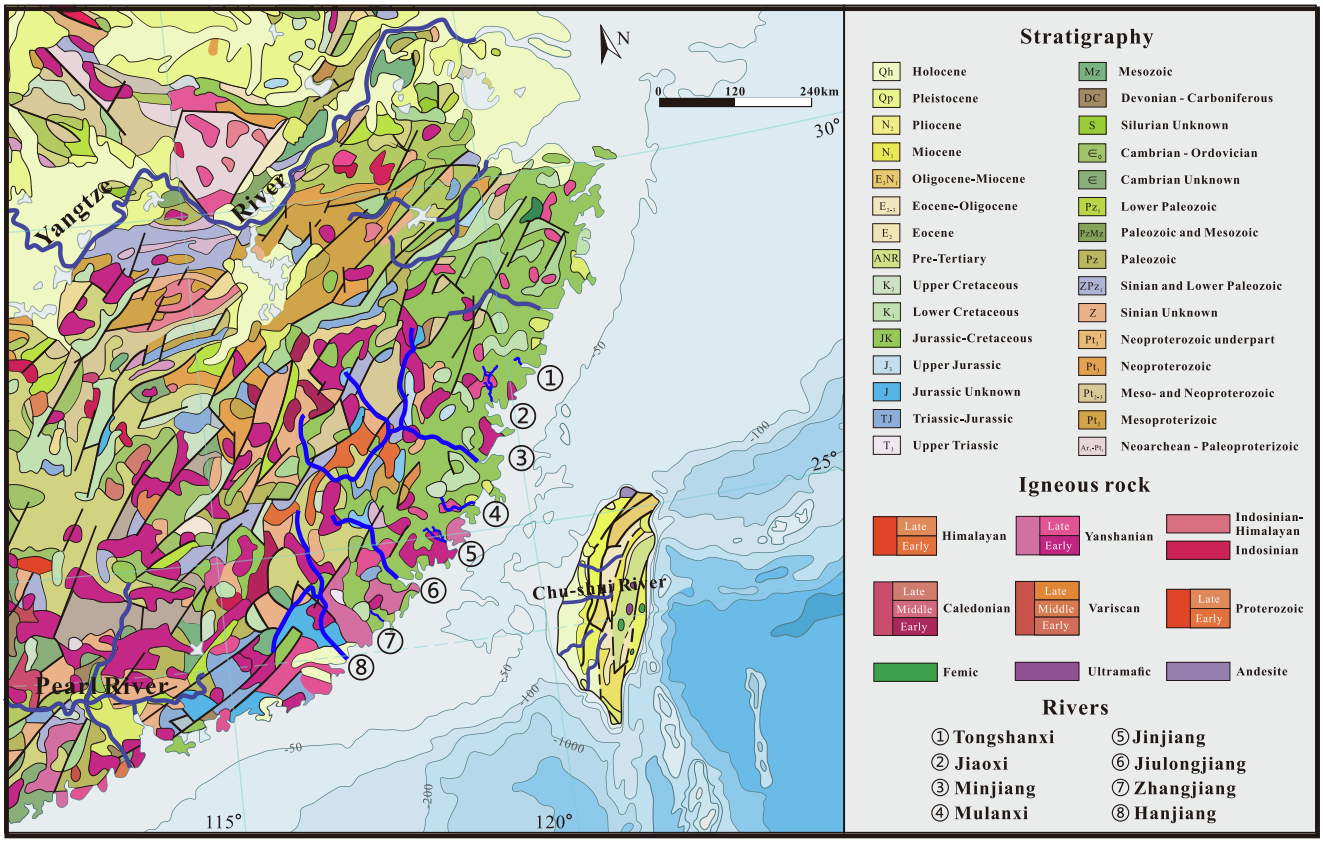

Fig. 2. Geological settings of the southeastern China, modified from Shen et al. (2021).

sedimentary rocks and Mesozoic igneous rocks (Fig. 2). In addition, the coastal zone in this region is significantly affected by strong tide with the maximum tidal range of more than 7 m (Wang et al., 2011; Lin, 2014; Wan et al., 2014; Wang et al., 2020; Li et al., 2021c). Based on the drainage area, these mountainous rivers can be classified into two types: small mountainous rivers (drainage area < 10000 km^2, including Tongshanxi River, Jiaoxi River, Mulanxi River, Jinjiang River and Zhangjiang River) and mesoscale mountainous rivers (drainage area $>$ 10000 km^2 and < 80000 km^2, including Minjiang River, Jiulongjiang River and Hanjiang River) (Fig. 1B).

These catchments have various bedrock lithological compositions (Table 1). On a whole, bedrock in small mountainous river basins consists of more clastic rocks, fewer granites and fewer metamorphic rocks than that in those mesoscale mountainous rivers (Table 1; Figs. 3–4). The bedrock lithology features of these eight rivers are illustrated in Figs. 3–4 and related quantitative calculation results are shown in Table 1.

3. Materials and Methods

3.1. Sampling

All the riverbed surface sediment samples were collected in river channels or along the banks in dry seasons (October to March). Specifically, the Minjiang River samples were obtained during October–December in 2016; the Hanjiang River samples were collected in March 2017; samples of other studied rivers were obtained in November 2019. Sampling locations are away from mining, quarrying and densely populated banks which are vulnerable to human activities. A few centimeters of the surface layer which are susceptible to dust were removed when sampling. Seafloor surface sediment samples from the Xiamen Bay and Dongshan Bay were collected by a grab sampler in July 2018.

3.2. Clay mineral analysis

Clay mineralogical analysis was performed following the procedures described by Mei et al. (2021). Samples were first placed in 100 ml centrifuge tube and soaked with pure water. And then the sediment–-water mixture was oscillated for 30 min. Sodium hexametaphosphate was added to prevent clay flocculation. The clay fractions (< 2 μm) were extracted by gravitational sedimentation according to the Stokes' law. Organic matter and carbonate were removed from the separated clay fractions by 10 % H_2O_2 and 1 mol/L CH_3COOH under 60 ℃ water bath, respectively. Clay particles were obtained after centrifugation and removal of the supernatant and were then suspended (dispersed by ultrasonic treatment), pipetted and deposited onto a glass slide and allowed to air-dry at room temperature. The clay mineral compositions of these oriented tablets were then determined in the following conditions: air-dried (N), ethylene glycol-solvated (EG) and heated to 500 °C for 2 h (T), using a Rigaku Ultima IV X-ray diffractometer (XRD). All samples were scanned from 4°–35° at a scanning speed of 4°/min under 40 kV, 30 mA, wavelength of 1.5406 and step width of 0.02° conditions.

The JADE 6.0 software was used to analyze the obtained XRD patterns (Fig. S1). Illite is generally identified by peaks at 10 Å (001), 5 Å (002) and 3.33 Å (003) on the N-treated diffractogram with no changes after being treated with ethylene glycol (Fig. S1). The (001) peak of kaolinite (7.2 Å) and the (002) peak of chlorite (7.1 Å) almost coincide on the EG-treated diffractogram (Fig. S1). They can be distinguished by the (002) peak (3.58 Å) of kaolinite and (004) peak (3.54 Å) of chlorite (Fig. S1). After heated to 500 ℃, the intensity of peaks of kaolinite decreases (Fig. S1). In addition, chlorite can also be recognized by peaks at 14.2 Å (001) and 4.74 Å (003) on EG-treated diffractogram (Fig. S1). Smectite can be identified by a combination of the N- and EG-treated diffractograms. The peak of smectite from 12 Å to 15 Å on the N-treated diffractogram will move to 17 Å (001) after being treated with

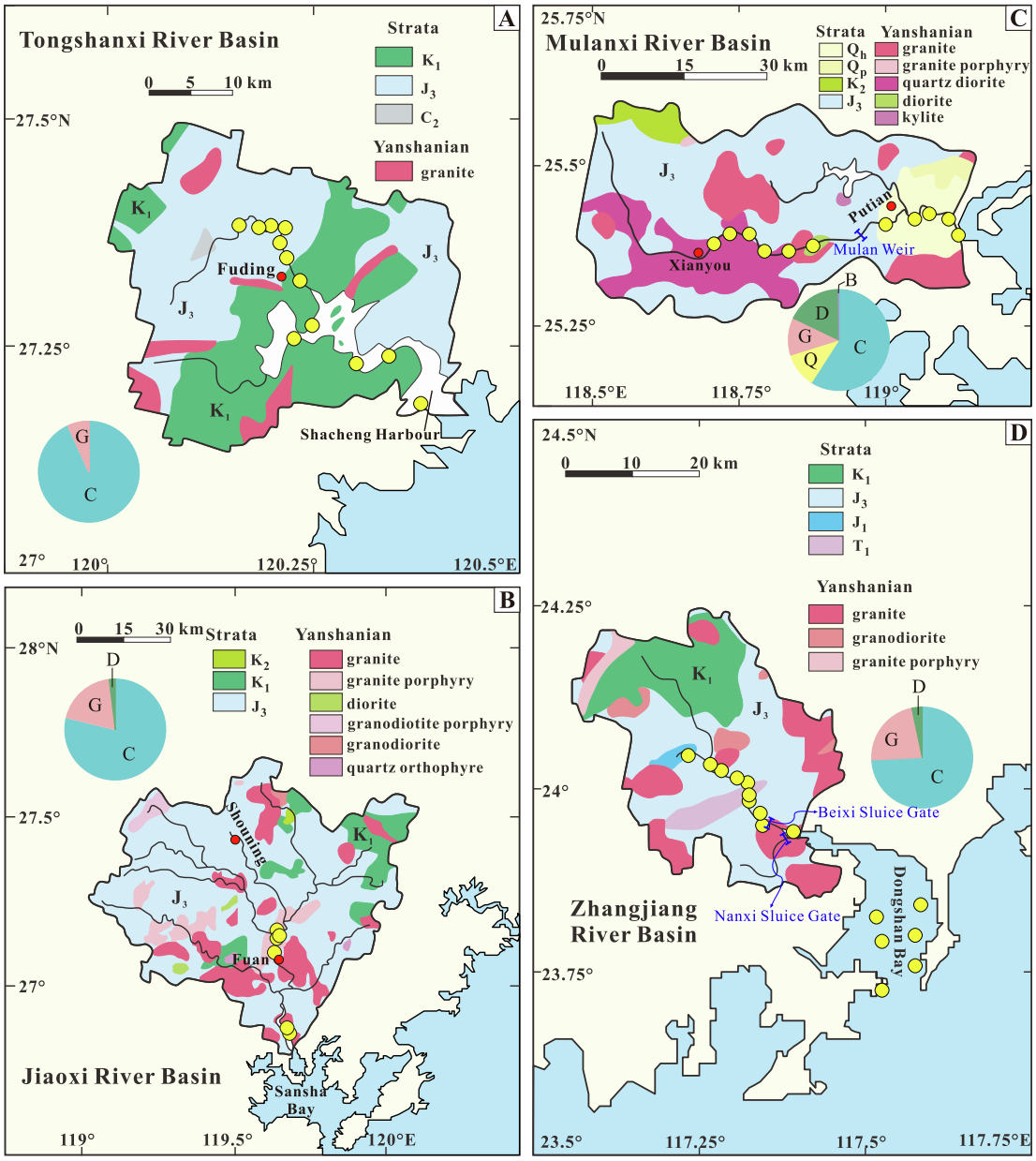

Fig. 3. Geological settings of the Tongshanxi River, Jiaoxi River, Mulanxi River and Zhangjiang River with sampling locations. To quantify lithology of river basins, we first defined the catchment area for each river basin and tributary using the ArcGIS 10.8 software and then drew geological maps for each watershed based on China Geological Map. After that, MATLAB software was used to calculate the proportion of each kind of bedrock lithology in the upper watershed represented by each sample. The pie chart shows the results of lithological quantification of each river basin. The C, Q, G, D and B in pie chart represent clastic rocks (volcano-sedimentary rocks and sedimentary rocks), Quaternary sediments, sum of granite, granite porphyry and quartz orthophyre, sum of diorite, quartz diorite, granodiorite and granodiorite porphyry, and basic rocks, respectively.

ethylene glycol (Fig. S1). After heated to 500 ℃ for 2 h, the peak of smectite collapses (Fig. S1). Semi-quantitative estimations of the relative percentages of clay minerals were based on the peak area (Biscaye, 1965) on XRD patterns of the EG-treated samples. The relative abundances of clay minerals were determined by the formula: 4 × I (illite 10 Å) + I (smectite 17 Å) + 2 × I (kaolinite, chlorite 7.1 Å) = 100 % (Biscaye, 1965; Khan et al., 2019). The relative proportions of kaolinite and chlorite were determined by using the ratio of the 3.58 Å and 3.54 Å peak areas (Fig. S1). In addition, all the previously reported clay mineralogical data compiled in this study (see Table 2 for details) were either calculated by the method of Biscaye (1965) (e.g., Xu et al. (2009)) or recalculated using the method of Biscaye (1965) if this method was not used (e.g., Liu et al. (2016)), so that the results can be directly compared.

3.3. Clay mineralogical proxies

Clay mineralogical proxies, i.e., illite chemistry index, illite crystallinity index and the ratio of kaolinite/illite (Ka/I), have been widely applied to evaluate sediment chemical weathering intensity and to trace sedimentary provenance (Liu et al., 2007b; Liu et al., 2011; Hu et al., 2014; Nayak et al., 2022). The illite chemistry index (illite 5 Å/10 Å) was defined as the ratio of the 5 Å and 10 Å peak areas on XRD patterns (Esquevin, 1969). The illite crystallinity index (Kübler Index) was considered as the value of the full width half maximum (FWHM) of the 10 Å peak. Values of illite chemistry index lower and higher than 0.40 represent Fe-Mg-rich illite and Al-rich illite, respectively. The former implies weak chemical weathering, whereas the latter represents strong hydrolysis (Hu et al., 2014; Wang et al., 2016; Yu et al., 2020). Low

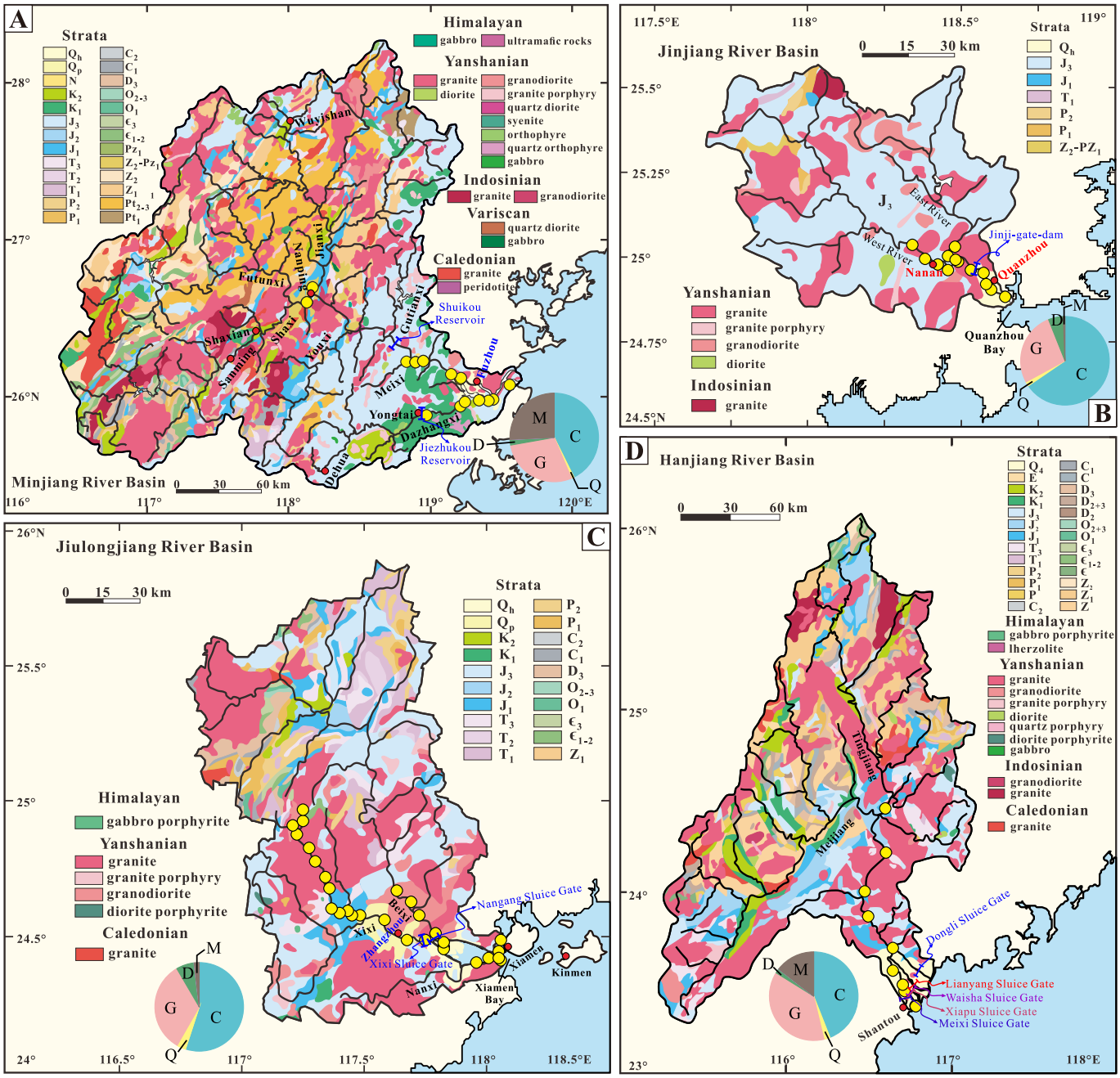

Fig. 4. Geological settings of the Minjiang River, Jiulongjiang River, Jinjiang River and Hanjiang River with sampling locations. The pie chart shows the results of lithological quantification of each river basin. The C, Q, G, D and M in pie chart represent clastic rocks (volcano-sedimentary rocks and sedimentary rocks), Quaternary sediments, sum of granite, granite porphyry, syenite, orthophyre, quartz orthophyre and quartz porphyry, sum of diorite, quartz diorite, granodiorite and diorite porphyrite, and metamorphic rocks, respectively.

values of illite crystallinity index represent well-crystallized illite, which is ideally regarded as a feature of weak hydrolysis for detrital illite. On the contrary, high values of illite crystallinity index represent poor crystallinity and thus may indicate intensive weathering conditions (Wang et al., 2016). As kaolinite and illite are generally considered as silicate weathering products of different stages (Nesbitt et al., 1997; Galán, 2006; Dill, 2017; Jian et al., 2019), high Ka/I values show strong chemical weathering (Liu et al., 2007b; Mei et al., 2021).

3.4. Geospatial analysis and statistics

In order to examine relationships between clay mineralogical proxies and possible controlling factors (MAT, MAP, lithology, mean basin slope), we carried out Pearson correlation analysis (Fig. S2). Additionally, we carried out the partial correlation analysis by MATLAB to test the correlations between clay mineralogical proxies and the individual factors. Data of clay mineralogical proxies are mean values of each river from this study (Table 2). Data of MAT and MAP are from Peng (2019, 2020), representing average values for the entire basin and are calculated from averages of the range of 1981 to 2021. The datasets are provided by the National Tibetan Data Center (http://data.tpdc.ac.cn). To quantify lithology of the river basins, we first defined the catchment area for each river basin and tributaries using the ArcGIS 10.8 software and then drew geological maps for each watershed based on the China Geological Map (1:1500000). After that, the MATLAB software was used to calculate the proportion of each kind of bedrock lithology of the river

Table 2
Average and range (in brackets) of clay mineral compositions of related riverbed and seafloor surface sediments in this study.

	Clay mineral assemblage											Illite chemistry index	SD	N	Illite crystallinity index	SD	N
	Smectite (%)	SD	Illite (%)	SD	Kaolinite (%)	SD	Chlorite (%)	SD	Ka/I	SD	N						
Tongshanxi River	0 (0–2)	1	47 (29–66)	13	34 (14–55)	14	19 (12–24)	3	0.88 (0.21–1.76)	0.58	12	0.41 (0.20–0.80)	0.17	12	0.42 (0.29–0.58)	0.08	12
Jiaoxi River	1 (0–2)	1	50 (31–84)	21	32 (11–51)	16	18 (5–24)	7	0.84 (0.13–1.64)	0.63	6	0.39 (0.26–0.48)	0.09	6	0.39 (0.34–0.46)	0.04	6
Minjiang River	0 (0–3)	1	32 (21–47)	6	47 (37–54)	5	21 (15–28)	3	1.53 (0.78–2.50)	0.47	18	0.64 (0.42–1.13)	0.21	18	0.43 (0.36–0.50)	0.04	18
Mulanxi River	2 (0–6)	2	36 (13–57)	17	39 (20–61)	17	23 (18–31)	4	1.68 (0.36–4.55)	1.53	11	0.45 (0.26–0.81)	0.16	11	0.33 (0.30–0.36)	0.02	11
Jinjiang River	0 (0–1)	0	23 (11–40)	9	56 (37–71)	10	20 (15–26)	3	2.93 (0.92–6.42)	1.58	13	0.62 (0.34–0.90)	0.16	13	0.37 (0.32–0.45)	0.05	13
Jiulongjiang River	0 (0–1)	0	21 (6–50)	12	56 (25–75)	12	22 (13–31)	4	3.82 (0.50–12.74)	2.89	23	0.66 (0.31–1.31)	0.21	23	0.42 (0.31–0.62)	0.08	23
Zhangjiang River	0 (0–0)	0	22 (6–44)	10	56 (32–67)	10	22 (17–30)	4	3.41 (0.74–9.96)	2.59	10	1.07 (0.52–2.30)	0.49	10	0.33 (0.29–0.39)	0.03	10
Hanjiang River	0 (0–4)	1	35 (10–51)	11	46 (30–67)	9	19 (13–25)	4	1.74 (0.71–6.78)	1.71	11	0.61 (0.31–1.84)	0.42	11	0.37 (0.29–0.54)	0.08	11
Quanzhou Bay*	4 (0–6)	2	61 (58–65)	3	19 (12–25)	5	16 (14–17)	1	0.31 (0.18–0.41)	0.09	6						
Xiamen Bay**	3 (0–7)	3	53 (35–67)	10	21 (12–39)	11	22 (11–27)	4	0.45 (0.20–1.09)	0.32	16	0.49 (0.42–0.64)	0.08	6	0.38 (0.35–0.43)	0.03	6
Dongshan Bay	1 (0–2)	1	46 (39–56)	8	28 (22–35)	5	25 (22–28)	3	0.64 (0.40–0.91)	0.20	6	0.45 (0.34–0.56)	0.08	6	0.36 (0.28–0.43)	0.05	6
Yangtze River*	3 (0–26)	3	70 (20–90)	14	14 (1–55)	9	14 (2–34)	7	0.27 (0.02–2.34)	0.37	135	0.49 (0.20–2.14)	0.29	131	0.55 (0.44–0.83)	0.09	75
Qiantangjiang River*	5 (1–12)	4	67 (59–76)	5	15 (7–23)	4	14 (7–20)	6	0.22 (0.12–0.35)	0.06	16						
Oujiang River*	6 (2–12)	3	71 (58–81)	5	10 (7–21)	3	13 (10–18)	2	0.14 (0.09–0.36)	0.05	54						
Taiwanese rivers*	1 (0–6)	1	73 (59–84)	5	2 (0–11)	3	25 (13–32)	4	0.03 (0.00–0.17)	0.04	78	0.35 (0.26–0.40)	0.03	52	0.16 (0.12–0.23)	0.03	61
Pearl River*	1 (0–4)	1	41 (11–60)	12	37 (24–63)	10	21 (10–35)	6	1.14 (0.43–5.58)	0.95	37	0.62 (0.45–0.8)	0.09	37	0.30 (0.24–0.42)	0.05	37
Guangxi rivers*	1 (0–2)	0	29 (22–37)	6	57 (46–65)	7	13 (9–18)	4	2.06 (1.25–3.00)	0.64	5						
Hainan rivers*	3 (0–7)	2	22 (13–45)	10	70 (46–80)	11	5 (4–6)	1	3.70 (1.02–5.93)	1.57	9	0.68 (0.36–1.18)	0.21	53	0.38 (0.27–0.81)	0.09	53
Luzon rivers*	76 (42–94)	13	2 (0–11)	1	15 (0–55)	12	8 (0–52)	12			35						
ECS shelf*	9 (2–16)	3	63 (47–71)	5	13 (5–24)	3	15 (6–26)	2	0.21 (0.09–0.41)	0.06	84				0.51 (0.41–0.68)	0.06	50
Taiwan Strait*	4 (0–18)	3	71 (35–85)	5	6 (0–41)	5	19 (6–29)	4	0.09 (0.00–1.18)	0.09	678	0.35 (0.28–0.44)	0.02	146	0.16 (0.14–0.21)	0.01	146
Guangdong offshore*	6 (0–28)	6	49 (37–58)	7	26 (12–38)	7	19 (14–25)	3	0.56 (0.21–1.00)	0.22	27						

Data without * are from this study. Data marked by * are published data: the Quanzhou Bay from Li et al., 2021b; the Yangtze River from He et al. (2013), Zhao et al. (2018), An et al. (2020) and Wang et al. (2021); Qiantangjiang River from Xu et al. (2009), Liu et al. (2016) and Xi et al. (2016); Oujiang River from Yang (1995), Xu et al. (2009) and Liu et al. (2016); Taiwanese rivers from Liu et al. (2008, 2010, 2016) and Wang et al. (2016); Pearl River from Liu et al. (2007b); Guangxi rivers from Liu et al. (2016); Hainan rivers from Hu et al. (2014) and Liu et al. (2016); Luzon rivers from Liu et al. (2009); the East China Sea (ESC) shelf from Youn et al. (2007) and Zhao et al. (2018); Taiwan Strait from Liu et al. (2008, 2010, 2016), Wang et al. (2016) and Li et al. (2021b); Guangdong offshore from Liu et al. (2007a, 2010, 2016). Data marked by **are from both this study and Li et al. (2021b). SD: standard deviation.

basin and of the upper watershed represented by each sample. The pie charts in Figs. 3–4 show the results of lithological quantification of each river basin. Mean basin slope was calculated by ArcGIS 10.8 based on the 90-m resolution Digital Elevation Model (DEM) (https://srtm.csi.cgiar.org) and the results were shown in Table 1.

4. Results

4.1. Clay mineral compositions of sediments from the studied rivers and estuarine bays

The clay mineral assemblages of surface sediments from the studied small–mesoscale mountainous rivers are mainly composed of kaolinite (11%–75%), illite (6%–84%) and subordinate chlorite (5%–31%) with scarce smectite (0%–6%) (Table 2; Table S1; Fig. 5; Figs. S3–S4). Smectite occurs only in sediment samples from the lower reaches close to estuary (Figs. S3–S4). From north to south, sediment samples from small mountainous rivers show increasing kaolinite content and decreasing illite content (Table 2; Fig. 5B). Values of the illite chemistry index of the small mountainous river sediments are between 0.20 and 2.30, with an average of 0.60 (Table 2; Table S1; Fig. 6A) and values of illite crystallinity index fall in the range of 0.29–0.58°Δ2θ, with an average of 0.37°Δ2θ (Table 2; Table S1; Fig. 6A). Values of the illite chemistry index of the mesoscale mountainous rivers vary greatly, from 0.31 to 1.84 with an average of 0.65 (Table 2; Table S1; Fig. 6A) and values of illite crystallinity index vary in the range of 0.29–0.62°Δ2θ, with an average of 0.41°Δ2θ (Table 2; Table S1; Fig. 6A). Clay minerals of the seafloor surface sediment samples from the Xiamen Bay and Dongshan Bay are mainly composed of illite (35%–67%), kaolinite (12%–39%) and chlorite (11%–28%) with scare smectite (0%–7%) (Table 2; Table S1; Fig. S3D; Fig. S4C; Fig. 5). Values of illite chemistry index of bay sediments vary from 0.34 to 64 with an average of 0.47 (Table 2; Table S1; Fig. 7F–G) and values of illite crystallinity index range from 0.28°Δ2θ to 0.43°Δ2θ, with an average of 0.37°Δ2θ (Table 2; Table S1).

4.2. Spatial differences in clay mineral compositions of sediments

On the whole, kaolinite and illite are the dominant clay minerals in all the studied surface sediment samples, together close to or larger than 80 % (Table 2; Table S1; Figs. S3–S4). Additionally, kaolinite and illite contents show remarkable differences among the studied rivers (Table 2;

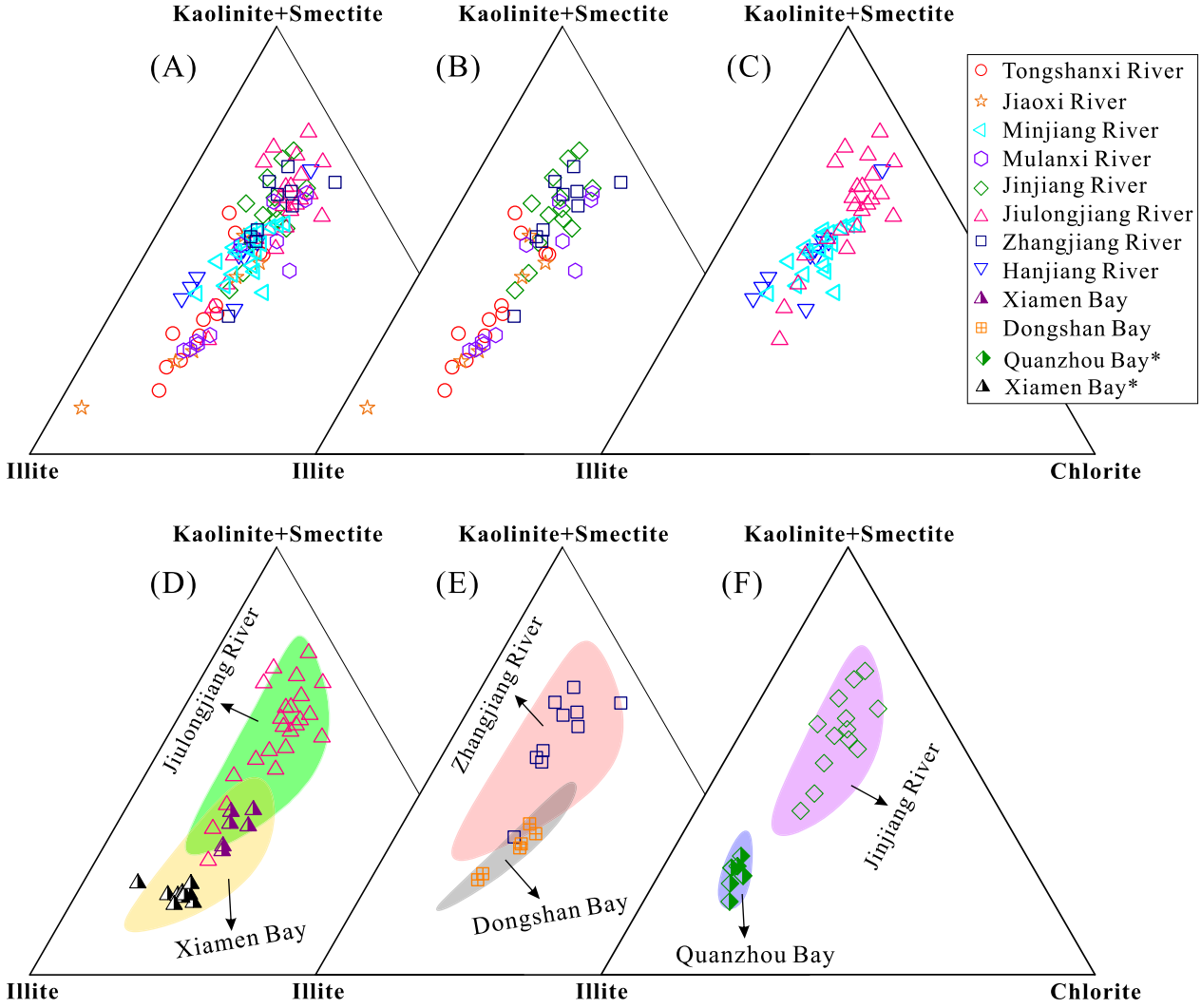

Fig. 5. Ternary diagram of the major clay mineral groups kaolinite + smectite, illite, and chlorite. (A) all the studied rivers; (B) small mountainous rivers; (C) mesoscale mountainous rivers; (D) comparison between the Jiulongjiang River and Xiamen Bay; (E) comparison between the Zhangjiang River and Dongshan Bay; (F) comparison between the Jinjiang River and Quanzhou Bay. Data marked by * are from Li et al. (2021b). Ninety-five percent confidence of clay mineral compositions of the Jiulongjiang River, Zhangjiang River, Jinjiang River, Xiamen Bay, Dongshan Bay and Quanzhou Bay were calculated and illustrated by ellipsoids with different color in D, E and F in ternary diagrams.

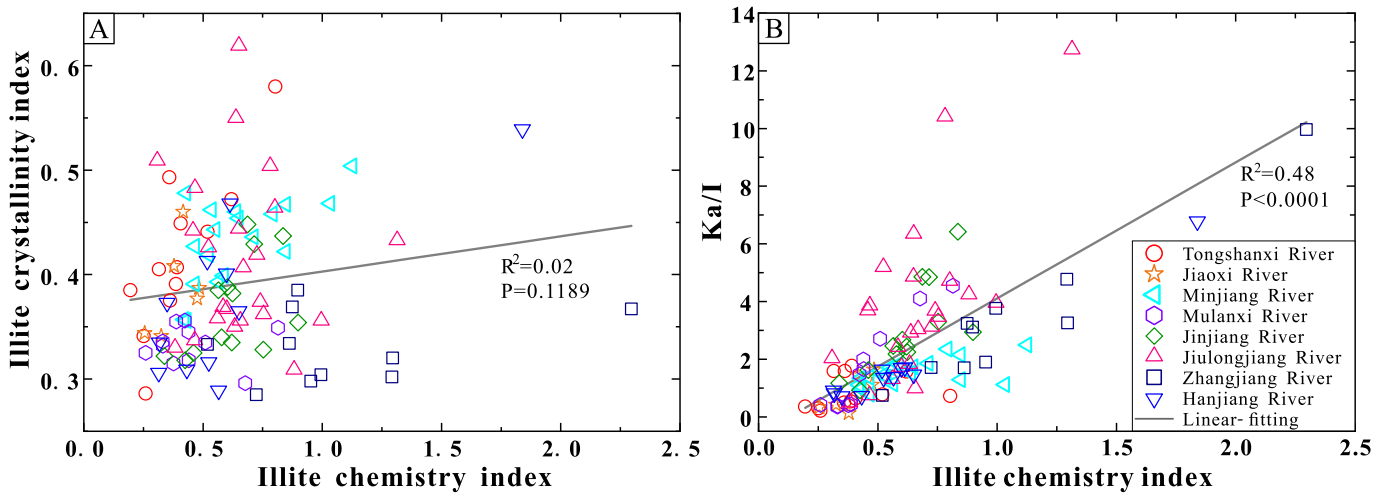

Fig. 6. (A) Correlation between the illite crystallinity index and the illite chemistry index of sediment samples from the investigated small–mesoscale mountainous rivers. (B) Correlation between Ka/I and illite chemistry index of sediments samples from the investigated small–mesoscale mountainous rivers. The illite chemistry index (illite 5 Å/10 Å) was defined as the ratio of the 5 Å and 10 Å peak areas. The illite crystallinity index (Kübler Index) was considered as the value of the full width half maximum (FWHM) of the 10 Å peak. Note that there is no correlation between illite crystallinity index and illite chemistry index, but Ka/I is positively correlated with illite chemistry index which might question illite crystallinity index as a chemical weathering index.

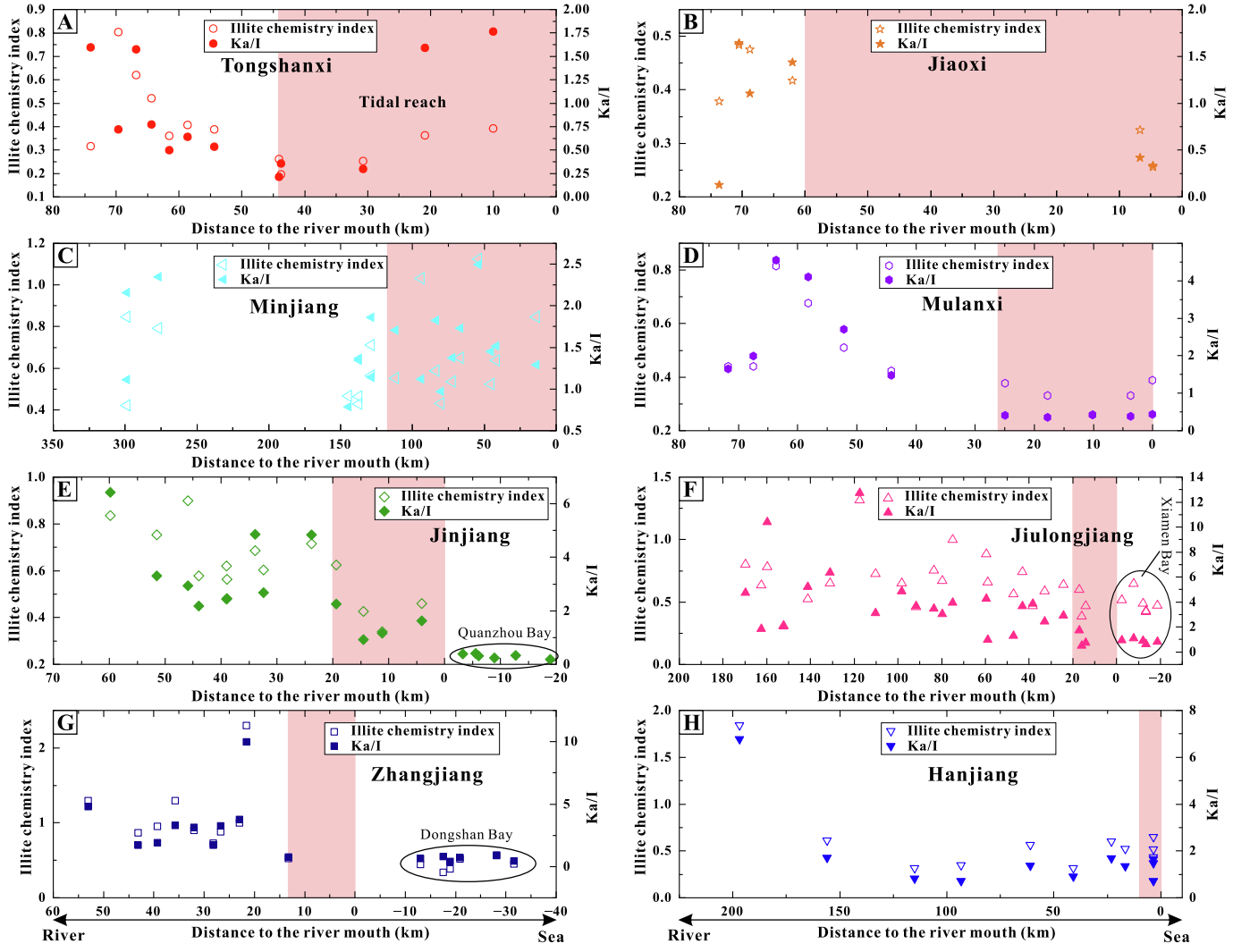

Fig. 7. Variations of illite chemistry index and the ratio of kaolinite/illite (Ka/I) with the distance to the river mouth. The rectangles with pink shades are length of tidal reach. Data of the Quanzhou Bay are from Li et al. (2021b). (For interpretation of the references to color in this figure legend, the reader is referred to the web version of this article.).

Figs. S3–S4; Figs. 5–6). As a result, the values of Ka/I vary greatly, from 0.13 (a sample from the Jiaoxi River) to 12.74 (a sample from the Jiulongjiang River) (Fig. 6B; Fig. 7). The content of kaolinite has a certain latitudinal zonation in those small rivers, but it is not obvious in the mesoscale rivers (Table 2; Fig. 5B–C). For the small mountainous rivers, kaolinite contents in the Zhangjiang River and Jinjiang River sediment samples are similar but higher than those in the Mulanxi River, Jiaoxi River and Tongshanxi River sediment samples (Table 2; Table S1; Figs. S3–S4; Fig. 5; Fig. 8A). For the mesoscale mountainous rivers, kaolinite contents are relatively high and tend to be higher than illite (Table 2; Fig. S4; Figs. 5–6). Kaolinite contents in the Minjiang River and Hanjiang River sediments are similar but lower than those in the Jiulongjiang River sediments (Table 2; Table S1; Fig. S4; Figs. 5–6; Fig. 8A). In addition to these differences among rivers, our data also show that clay mineral compositions in the upper and lower reaches of the same river (e.g., Tongshanxi River, Jiaoxi River, Mulanxi River and Jinjiang River) also vary significantly (Figs. S3–S4; Fig. 7). Specifically, the values of both Ka/I and illite chemistry index show obvious decreasing trends downstream (Fig. 7). Values of the illite crystallinity index are also diverse, but are uncorrelated with the illite chemistry index (Fig. 6A).

Our results also show significant heterogeneity of clay mineral compositions in surface sediments among river non-tidal influenced reaches, tidal reaches and related estuarine bay areas (Figs. S3–S4; Fig. 5D–F; Fig. 7; Fig. 9). Kaolinite contents in most samples of the Zhangjiang River basin, Jiulongjiang River basin and Jinjiang River basin are higher than those of the corresponding Dongshan Bay, Xiamen Bay and Quanzhou Bay, respectively (Fig. S3D; Fig. S4B–C; Fig. 5D–F; Fig. 7E–G). On the contrary, illite contents are higher in these bays than those in the related river catchments (Fig. S3D; Fig. S4B–C; Fig. 5D–F; Fig. 7E–G). Additionally, smectite is mostly identified in sediments from the tidal reaches and bays (Figs. S3–S4; Fig. 9). Similarly, values of the illite chemistry index show great heterogeneity between the tidal reaches and non-tidal influenced reaches, with lower values of illite chemistry index in the tidal reaches than those in the non-tidal influenced reaches, except the Tongshanxi River (Fig. 7). It is worth noting that values of the illite chemistry index and Ka/I in the tidal reaches are relatively more homogeneous than those in the non-tidal influenced river reaches (Fig. 7; Fig. 9) and are similar to those in the related estuarine bays (Fig. 7E–G; Fig. 9).

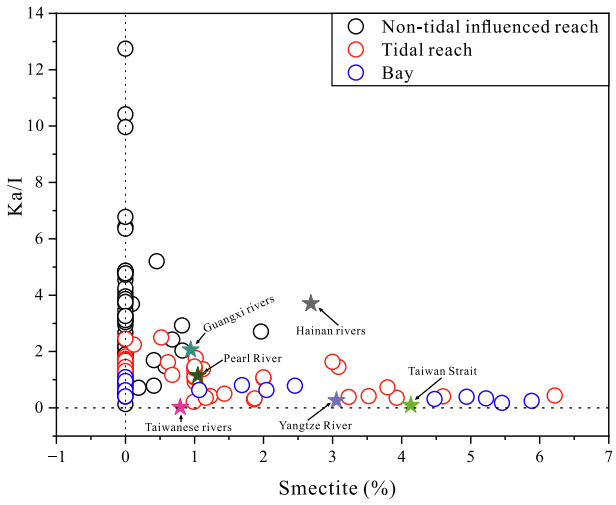

Fig. 9. The ratio of kaolinite/illite (Ka/I) vs. smectite content binary plots. It is worth noting that values of Ka/I decrease but the smectite contents increase from the non-tidal influenced reaches to tidal reaches and then to bays.

4.3. *Correlation between clay mineralogical proxies and possible controlling factors*

The Pearson analysis results show that Ka/I is strongly negatively correlated with MAP and illite chemistry index is moderately negatively correlated with MAP (Fig. S2). By contrast, both Ka/I and illite chemistry index are strongly positively correlated with MAT (Fig. S2). Positive correlation between Ka/I and the percentage of intermediate-acid igneous rocks is stronger than correlation between illite chemistry index and the percentage of intermediate-acid igneous rocks (Fig. S2). Both Ka/I and illite chemistry index have weak negative correlations with the percentage of clastic sedimentary rocks and mean basin slope (Fig. S2).

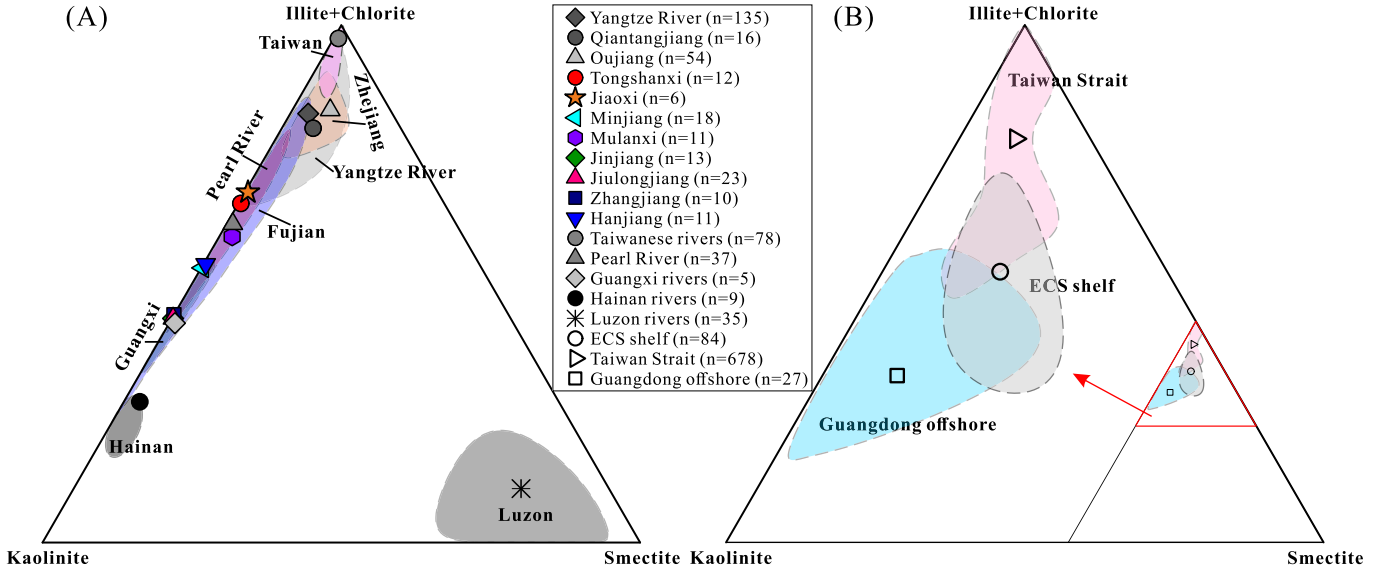

Fig. 8. Ternary diagram of smectite-(illite + chlorite)-kaolinite. (A) Fluvial samples (surface + suspended). (B) Seafloor surface samples. Published data of river samples: the Yangtze River from He et al. (2013), Zhao et al. (2018), An et al. (2020) and Wang et al. (2021); Qiantangjiang River from Xu et al. (2009), Liu et al. (2016) and Xi et al. (2016); Oujiang River from Yang (1995), Xu et al. (2009) and Liu et al. (2016); Taiwanese rivers from Liu et al. (2008, 2010, 2016) and Wang et al. (2016); Pearl River from Liu et al. (2007b); Guangxi rivers from Liu et al. (2016); Hainan rivers from Liu et al. (2016); Luzon rivers from Liu et al. (2009). Published data of seafloor samples: the East China Sea (ESC) shelf from Youn et al. (2007) and Zhao et al. (2018); Taiwan Strait from Liu et al. (2008, 2010, 2016), Wang et al. (2016) and Li et al. (2021b); Guangdong offshore from Liu et al. (2007a, 2010, 2016).

The Pearson analysis results also show a strong correlation between climate and mean basin slope and a weak–moderate correlation between climate and lithology (Fig. S2). The weak–moderate correlation between climate and lithology may make the correlation between the clay mineralogical proxies and climate or lithology a spurious correlation. Therefore, partial correlation analysis was carried out among climate (MAP, MAT), lithology (percentage of intermediate-acid igneous rocks) and clay mineralogical proxies (Ka/I, illite chemistry index) (Table S2). Results of the partial correlation analysis indicate the true strong correlation between clay mineralogical proxies and climate, true moderate correlation between Ka/I and lithology, and weak correlation between illite chemistry index and lithology (Table S2).

The Pearson correlation analysis and partial correlation analysis for clay mineralogical proxies and environmental factors (Table S2; Fig. S2) indicate that climate factors (e.g., MAT, MAP) have the greatest influence on clay minerals of the studied river sediments, followed by lithology (percentage of intermediate-acid igneous rocks and clastic sedimentary rocks), and then by catchment geomorphology (mean basin slope).

5. Discussion

Sediments from the investigated small–mesoscale mountainous rivers show remarkable diversity in clay mineral compositions (Table 2; Figs. 5–10; Figs. S3–S4). Based on the results of Pearson analysis and partial correlation analysis, we find that climate may play a major role in controlling clay minerals, followed by bedrock lithology. The influence of catchment climate and bedrock lithology on clay minerals is stated in the following sections. Additionally, due to the strong influence of tidal currents in the study area and its location in a densely populated region, how tidal currents and human activities may impact the formation and transport process of clay minerals is also discussed.

5.1. Predominant climatic control on the clay mineral heterogeneity

Generally, climate plays an important role in clay mineral formation on the Earth's surface (Liu et al., 2016; Zhao et al., 2023; Lyu and Lu, 2024). Kaolinite is a preliminary weathering product under intense weathering in tropical or humid climates (Tabor and Myers, 2015; Liu et al., 2016; Pang et al., 2018). For example, high kaolinite content

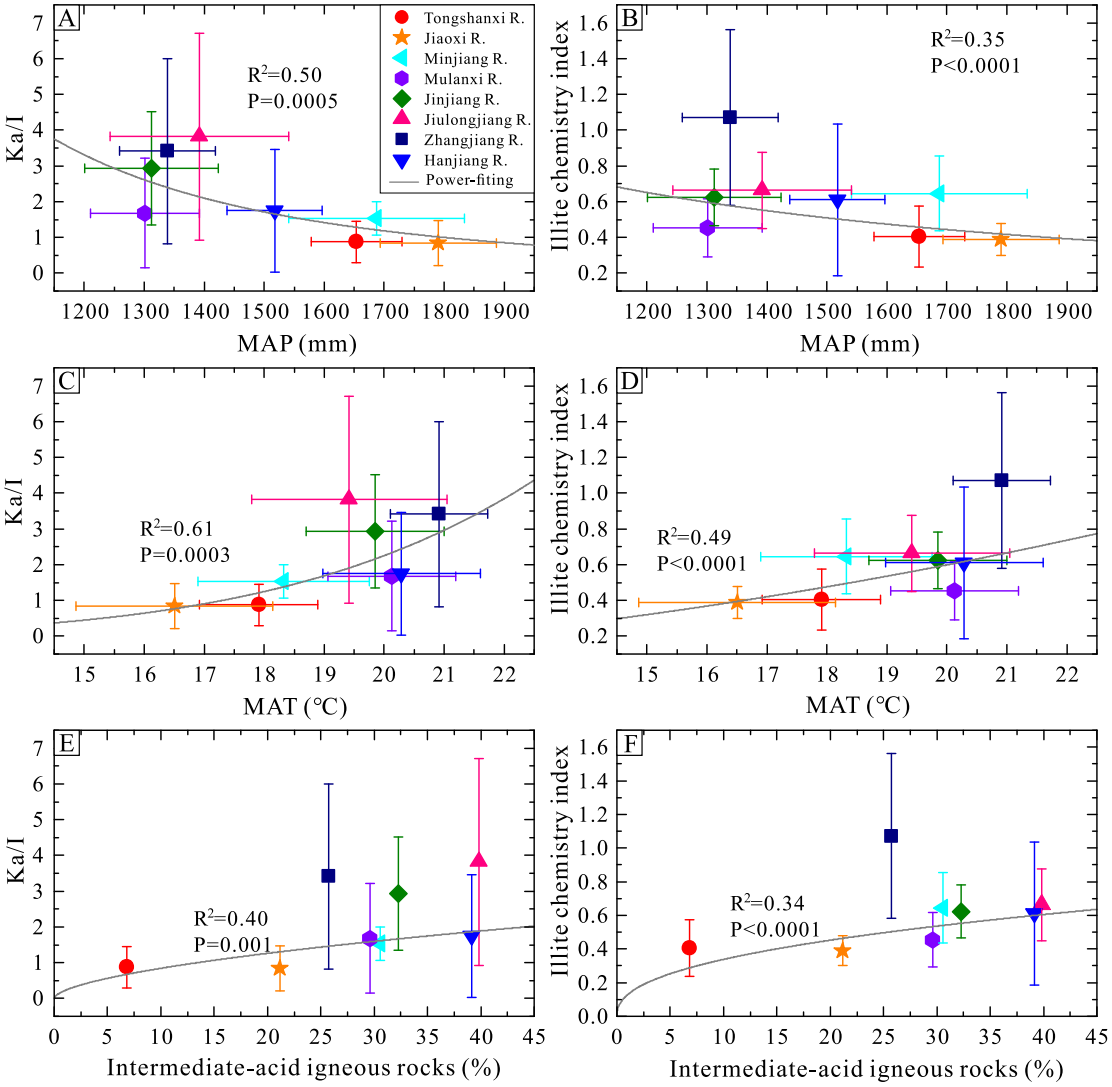

Fig. 10. Correlations of clay mineralogical proxies (illite chemistry index and Ka/I) with possible influencing factors (MAP, MAT, lithology) of the studied rivers. Note that MAT and proportion of intermediate-acid igneous rocks may promote the heterogeneity of clay mineral compositions. The intermediate-acid igneous rocks represent sum of granite, granite porphyry, syenite, orthophyre, quartz orthophyre, quartz porphyry, diorite, quartz diorite, granodiorite, diorite porphyrite and granodiorite porphyry. Power model fitting between factors (MAP, MAT and lithology) and clay mineralogical proxies (Ka/I and illite chemistry index) by Origin 2024b is shown as gray solid line.

(46%–80%) was detected in river sediments in Hainan and Guangxi, south China (Table 2; Fig. 8A; Liu et al., 2016). Illite and chlorite mainly arise from physical erosion-dominated regions where hydrolysis is limited by cold or arid climates (Pang et al., 2018; Deconinck et al., 2019; Khan et al., 2019). All the studied river basins are under a subtropical East Asian monsoon climate with abundant precipitation and warm temperature (Table 1; Fig. 1B). In addition, they are all well-vegetated by the dominant evergreen broadleaved forest (Yue et al., 2012). Such climate conditions are conducive to kaolinite generation, similar to the Pearl River catchment (Table 2; Fig. 8A), consistent with the moderate–high kaolinite contents in this study (Table 2; Fig. 5; Figs. S3–S4). Although all the studied river catchments are under the same climatic zone, their mean annual precipitation (MAP) and mean annual temperature (MAT) vary in different river catchments (Table 1; Fig. 10). We find that the values of Ka/I and illite chemistry index decrease with MAP values (Fig. 10A). The influence of precipitation on chemical weathering process is complex. Precipitation may increase chemical weathering intensity by supplying fluid for chemical reactions (e.g., Maher, 2010; Maher and Chamberlain, 2014) or weaken chemical weathering by driving erosion, such as storm-triggered mass wasting, and then decreasing soil residence time for reaction (Jian et al., 2020a; Deng et al., 2022). Although the negative correlations between chemical weathering intensity (based on clay mineralogical proxies) and MAP values are present here (Fig. S2; Fig. 10A–B), further studies are needed to unravel the subtropical precipitation-runoff-erosion-weathering mechanisms and to determine whether the monsoon and typhoon precipitation in these investigated regions may drive fast erosion and weaken chemical weathering in the mountainous catchments. Additionally, we also find that the values of Ka/I and illite chemistry index increase with MAT values (Fig. 10C–D), showing a potentially positive control of temperature on the chemical weathering processes associated with clay minerals (Fig. S2). Similar coupling relations between silicate chemical weathering intensity and temperature have been highlighted in several previous studies (Ren et al., 2020; Deng et al., 2022). Temperature dependence of weathering is thought to be expressed as an activation energy increase as transport, clay precipitation, disaggregation, and fracturing increasingly couple to dissolution (Brantley et al., 2023). Temperature may enhance the dissolution of feldspar to clay minerals which is viewed as the most common silicate weathering reaction (Deng et al., 2022).

5.2. Bedrock lithological control on the clay mineral heterogeneity

We find that the values of Ka/I show a positive correlation with the proportion of intermediate-acid igneous bedrock contents of different river basins (Table S2; Fig. S2), revealing possible bedrock lithological control on the clay mineral heterogeneity. In addition to the climate-dominated chemical weathering process, heterogeneity of clay mineral compositions caused by bedrock lithological diversity in the tributaries (Fig. S5) may explain the higher values of illite chemistry index and Ka/I in the upper reaches, compared with the lower reaches, such as the Jinjiang River. Furthermore, principal component analysis (PCA) results focusing on bedrock lithology and clay mineral compositions (Fig. S6) show a positive correlation between kaolinite contents and intermediate-acid igneous rocks and a positive correlation between illite content and clastic rocks, except for samples from the Tongshanxi River and Jinjiang River (Fig. S6). Such simplified and rough lithology classification based on geological maps may obscure the real relationship between clay mineral compositions of river sediments and bedrock lithology, but the attempt points to the potential lithological control on the clay mineral compositions.

Investigations on weathering profiles in Fujian Province show that kaolinite content is much higher than illite content (average of Ka/I > 8) in all layers of weathering profiles with intermediate-acid igneous rocks (Su et al., 2017; Mei et al., 2021; Wang, 2024). Intermediate-acid igneous rocks contain abundant plagioclase and K-feldspar which are easily weathered to kaolinite by rapid removal of K^+, Ca^{2+} and Na^+ under the warm and wet subtropical monsoon climate (Kim et al., 2017; Deng et al., 2022; Wang, 2024). On the contrary, illite content is much higher than kaolinite content (average of Ka/I < 0.5) in bedrock and saprolite of weathering profile with sedimentary rocks (fine-grained sandstone; Wang, 2024). Based on the clay mineral compositions and main bedrock lithology of the studied river basins, we infer that illite may originate from weak chemical weathering or physical erosion of clastic rocks in those catchments. In other words, illite may inherit from illite-rich sedimentary rocks (e.g., fine-grained sandstone from Wang (2024)).

A great number of previous studies have highlighted the lithological control on clay minerals in soils and river sediments. For example, abundant illite and chlorite contents are observed in sediments from the Taiwanese rivers (located in the same subtropical monsoon climate region as Fujian Province), which are probably due to insufficient chemical weathering of sedimentary and metasedimentary rocks or the inheritance of sedimentary bedrock terranes (i.e., detrital clay mineral recycling) (Fig. 8A; Liu et al., 2008, 2010, 2016; Liu et al., 2011; Wang et al., 2016; Zhang et al., 2022). Likewise, illite is thought to be derived from mica shist weathering but smectite and chlorite are from weathered volcanic effusive rocks in warm and humid Indonesia (Gingele et al., 2001). River sediments from the Luzon Island (tropical East Asia) have extremely high smectite contents (Fig. 8A). This is thought to be attributed to the majority of andesitic-basaltic volcanic and sedimentary rocks (Liu et al., 2009). It is widely accepted that mafic rocks tend to be weathered to smectite and further form kaolinite, whereas felsic rocks tend to be altered to illite and further form kaolinite (Liu et al., 2016; Zhao et al., 2023). Absence or extremely low abundances of mafic bedrock (Table 1; Figs. 3–4) in the study area may interpret the scarce smectite content in the non-tidal influenced reaches.

5.3. Tidal effects on clay mineral transport and deposition of the small–mesoscale mountainous rivers and estuarine bays

Our results show that values of the Ka/I and illite chemistry index vary greatly from the non-tidal influenced reaches to the tidal reaches and estuarine bays (Fig. 7). We note that clay mineral compositions in the tidal reaches and the related estuarine bays are more similar to those in the Fujian offshore of the Taiwan Strait than those in the related rivers (Table 2; Fig. 8B; Liu et al., 2008, 2010, 2016; Wang et al., 2016; Li et al., 2021b). Clay mineral compositions of sediments in the Taiwan Strait consist of abundant illite and chlorite with subordinate kaolinite and smectite (Table 2; Fig. 8B; Liu et al., 2008, 2010, 2016; Wang et al., 2016; Li et al., 2021b). Given the tiny size of detrital clay minerals and the strong tidal current along the SE China coast, we convince that variations in clay mineral compositions of the sediments from tidal reaches, especially for the small mountainous rivers, are dominantly caused by the river sediment mixing with the offshore sources. This mixing occurs due to strong tidal pumping which pumps seawater with fine-grained sediments into the river catchment. Carried by the Zhe-Min Coast Current, clays from the Yangtze River and the East China Sea (ESC) shelf (rich in illite and chlorite with more smectite than Zhe-Min rivers (Table 2; Fig. 8)) can reach the Fujian offshore (Xu et al., 2009). This effect is also observed in the Qiantangjiang River and Oujiang River (see Fig. 1B for locations) estuary regions (Table 2; Xu et al., 2009; Xi et al., 2016). The Taiwan Warm Current may transport clays from the Taiwanese rivers (rich in illite and chlorite (Table 2; Fig. 8)), such as the Cho-shui River and Kao-ping River, to the Fujian offshore (Li et al., 2021b; Shen et al., 2021). These transport processes of clay minerals make the fine-grained sediments in the Fujian offshore containing abundant illite and smectite. These illite- and smectite-bearing fine-grained sediments may be pumped into the tidal reaches of the Zhe-Min rivers under the influence of the strong tides (Liu et al., 2008, 2010, 2016; Wang et al., 2016). These processes result in well-mixed (i.e., relatively homogeneous) clay mineral compositions (Fig. 7) and thus

interfere with clay mineral signals of river catchments. This explains the phenomenon that smectite mostly occurs in bays and tidal reaches and why illite content is higher in bays and the tidal reaches than that in the non-tidal influenced reaches (Figs. S3–S4; Fig. 9). Tidal pumping effects are particularly pronounced in these small mountainous rivers, such as the Mulanxi river where clay mineral assemblages in tidal reach (from Mulan Weir to estuary) are almost invariable (Fig. S3C). The tidal pumping effects hypothesis is also supported by recent sediment element geochemical analysis results (Li et al., 2023). Consequently, our findings emphasize that surface sediment samples in tidal reaches, estuaries and bays with strong tidal influences cannot represent the average composition of particles eroded from the entire river catchment.

5.4. Potential influence of human activities on sediment transport of the small–mesoscale mountainous rivers

Human activities, such as dam and reservoir construction, land use and mining, can significantly impact river sediment source-to-sink processes (Vörösmarty et al., 2003; Wang et al., 2007; Chen et al., 2018; Gao et al., 2019). Dams and reservoirs were established in all the studied small–mesoscale mountainous river catchments (Fujian Province Water Management Institute, 2024) (http://slt.fujian.gov.cn). These artificial constructions are expected to trap sediments from the upstream regions (Dai et al., 2009; Yang and Yin, 2018). Provenance interpretations on Minjiang River-discharged suspended sediments indicate prominent contributions of the upstream rocks (Jian et al., 2020b). And seasonal variations were observed (Jian et al., 2020b). These findings suggest that dams and reservoirs may control modern sediment fluxes but do not have significant effects on sediment compositions (e.g., clay minerals) of the small–mesoscale mountainous rivers in Fujian Province. Nevertheless, quantification of hydroclimatic and anthropogenic contributions to sediment compositions and fluxes of these rivers is worthy of future consideration. However, we believe that dams and sluices building in lower reaches can block the upstream flow of tidal currents, artificially distinguishing between tidal and non-tidal influenced reaches. The typical dams and sluices include the Mulan Weir in Mulanxi River, Jinji-gate-dam in Jinjiang River, Xixi and Nangang Sluice Gate in Jiulongjiang River, Beijiang and Nanjiang Sluice Gate in Zhangjiang River and Dongli, Lianyang, Waisha, Xiapu and Meixi Sluice Gate in Hanjiang River (see Figs. 3–4 for locations). Because of these artificial blocks, extents of tidal reaches of these rivers are much smaller than those of rivers without dams and sluices in the downstream regions (Minjiang, Jiaoxi and Tongshanxi River) (Table 1). As a result, the interference of clay minerals from the Fujian offshore to the clay mineral signals from rivers is limited to a small area (Fig. 7D–H). Land use types of all the studied rivers are similar, characterized by mainly forest land and more farmland and construction land in the lower reaches than those in upper reaches (Gao et al., 2024) which is expected to reduce soil residence time and then decrease chemical weathering intensity in lower reaches (Vanacker et al., 2019). This might also account for the decreasing kaolinite from upstream regions to downstream regions.

5.5. Implications

5.5.1. Implications for sediment chemical weathering intensity evaluation based on clay mineralogy

The results in this study show that the values of illite chemistry index fit well with Ka/I values, but not with values of illite crystallinity index (Fig. 6). This might question illite crystallinity index as a chemical weathering index. Furthermore, we note that values of illite crystallinity index of sediments from the Yangtze River and Zhe-Min rivers (this study) are higher than those in the Pearl River (Fig. S7), which goes against the trend of chemical weathering intensity from high-latitude to low-latitude regions. This means that caution should be exercised while using the clay mineral compositions (and the proxies) of river sediments to indicate catchment chemical weathering intensity.

As mentioned above, bedrock lithology controls clay mineral compositions of the river sediments. We realize that illite in sediments can be the product of crystalline rock weathering and can also be directly supplied from illite-rich sedimentary rocks (Meunier and Velde, 2004). Sedimentary rocks are the common bedrock types in the investigated watersheds (Figs. 3–4). Illite crystallinity index of river sediments derived from ancient sedimentary rocks may not represent chemical weathering intensity during the latest sedimentary cycle, but represent the degree of diagenesis and even metamorphism of the sedimentary rocks (Warr and Ferreiro Mählmann, 2015; Warr and Cox, 2016; Austermann et al., 2021). This means that chemical weathering evaluation based on detrital illite crystallinity is unlikely to provide useful results for those river catchments with complex bedrock lithology. Lithological interference cannot be ignored even when using Ka/I and illite chemistry index to assess chemical weathering intensity (Fig. S5). How to distinguish the newly-formed and inherited illite remains challenging and is especially critical for those sedimentary bedrock-involved cases.

5.5.2. Implications for sediment source-to-sink system studies

Studies on the source-to-sink transport process of fluvial sediments have received much attention (e.g., He et al., 2013; Liu et al., 2016; Cao et al., 2019; Li et al., 2021b). Determining sediment output signatures for small–mesoscale mountainous rivers is challenging (e.g., Deng et al., 2019) but important to tracing continental margin sediment provenance. Sediments at outlets of small–mesoscale mountainous rivers are usually thought to represent the average composition of materials weathered and eroded from the entire river catchments (Li et al., 2023). Thus, most studies tend to target estuarine regions as common sampling sites for obtaining river provenance signals (e.g., Xu et al., 2009). However, the significant heterogeneity of clay minerals (Figs. 5–7; Fig. 10; this study), geochemical composition and provenance (Li et al., 2023), which may be integrated results from bedrock lithology, catchment climate and tidal effects (even human activities), drive us to reevaluate the current establishment on output signals of fine-grained sediments from the SE China coast mainland rivers (Fig. 11). Especially the contrasting bedrock lithology and the prevailing tidal water intrusion, increase the difficulty in obtaining the exact clay mineral information of terrigenous sediments (Fig. 11). We suggest sampling at the river mouth when the lowest tide level occurs and after extreme rainfall (depending on how long the river responds to the precipitation), so that the sediment samples may show the river signal to the greatest extent possible. Such a sampling strategy might provide a clear signal of riverine sources, especially when studying the provenance of fine-grained sediments. Sampling in non-tidal influenced areas ensures sediments representing terrigenous signals, but such sampling strategy may not cover enough information for those small mountainous rivers in strong tidal effect regions.

6. Conclusions

This contribution presents clay mineralogical analysis results for 116 riverbed sediment samples from eight small–mesoscale mountainous river basins with contrasting bedrock lithology and 12 sediment samples from two estuarine bays in the coastal area of SE China. Our results indicate that clay mineral heterogeneity of sediments is more notable than previously known, which may be attributed to the underrated differences in catchment climate and bedrock lithology. The relatively low heterogeneity in clay minerals from tidal reaches and estuarine bays is distinctively different from those from the non-tidal influenced reaches. This reveals the well-mixing of the offshore-sourced and mountain-supplied fine-grained sediments and highlights the major role of the tidal effects. Our findings suggest that the contrasting bedrock lithology and prevailing tidal water intrusion make it more challenging to obtain reliable output signals of terrigenous sediments for the Zhe-Min small–mesoscale mountainous rivers in SE China coast.

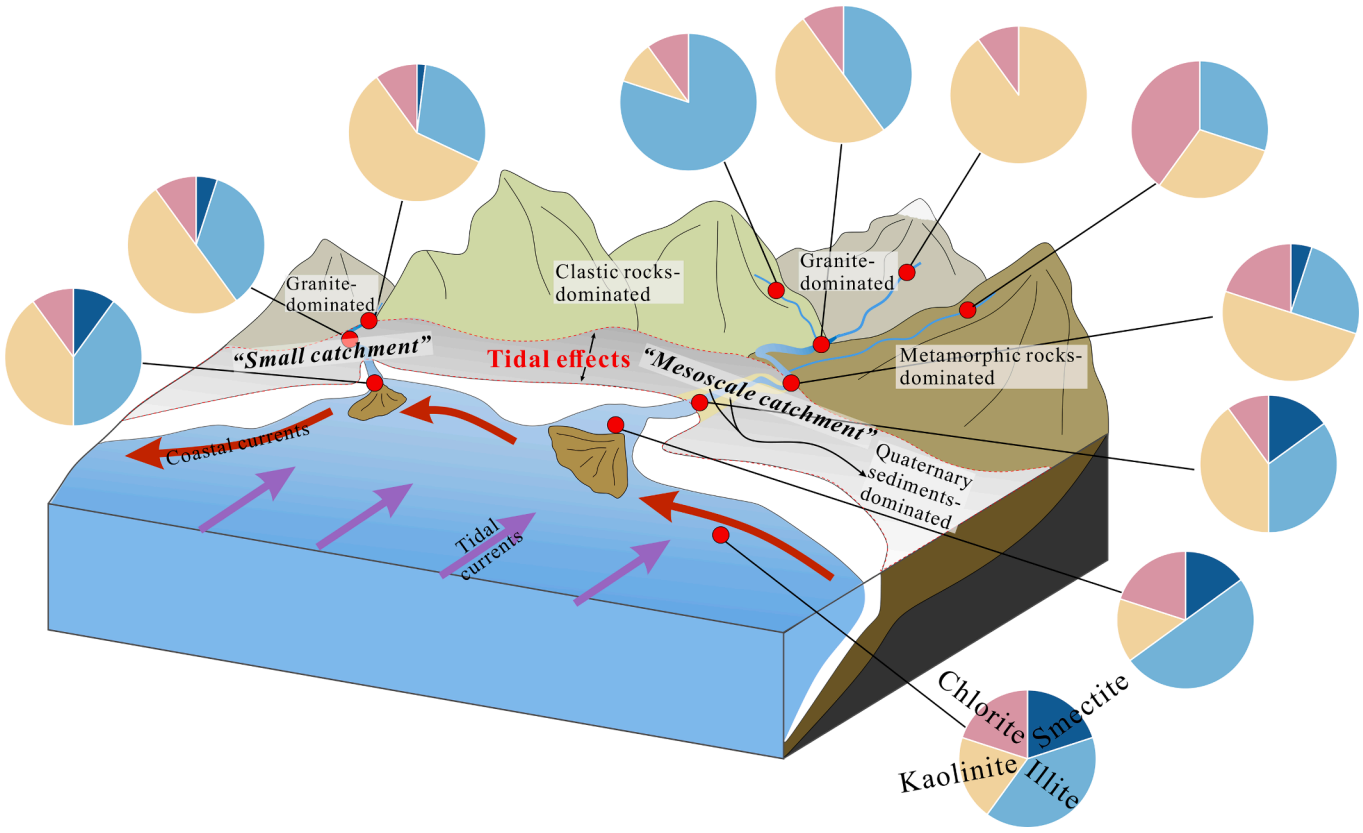

Fig. 11. Schematic clay source-to-sink model of small–mesoscale mountainous rivers showing influence of lithology, tides and ocean currents on clay mineral composition. Based on this study, we think that granite is easily weathered to kaolinite, clastic rocks are mainly weathered to illite, and metamorphic rocks can be altered mainly to chlorite with fewer kaolinite and illite. Here we assume that bedrock of river catchments cannot be altered to smectite (like this study) and smectite comes from offshore area. Thus, smectite content can be a proxy of tidal effects. When tributaries of different bedrock lithologies merge into the main stream, clay mineral compositions of sediments mix in the relatively large rivers (mesoscale catchment in this study). In the tidal reach, tides and currents will also pour water with fine-grained sediments into river, and thus clay mineral composition in estuary is a mixing product of river catchment and offshore area. For small river catchments, tidal effects are particularly strong, and even can reach upstream regions.

CRediT authorship contribution statement

Ling Wang: Writing – original draft, Investigation, Data curation, Conceptualization. **Xing Jian:** Writing – review & editing, Data curation, Conceptualization. **Haowei Mei:** Visualization, Investigation, Data curation, Conceptualization. **Xiaotian Shen:** Resources, Investigation, Data curation. **Hanjing Fu:** Resources, Investigation, Data curation.

Declaration of competing interest

The authors declare that they have no known competing financial interests or personal relationships that could have appeared to influence the work reported in this paper.

Acknowledgements

This research was supported by the National Science Foundation of Xiamen, China (No. 3502Z20227006) and the National Natural Science Foundation of China (Nos. 42476051, 41806052). We appreciate former graduate students (Hanghai Liang, Dongming Hong and Shuo Zhang) from Xiamen University for their help in field work and lab analysis. Acknowledgement goes to the Editor and the anonymous reviewers for critical and constructive feedbacks which were extremely helpful in improving earlier versions of this manuscript.

Appendix A. Supplementary data

Supplementary data to this article can be found online at https://doi.org/10.1016/j.catena.2024.108470.

Data availability

Data will be made available on request.

References

Adriaens, R., Zeelmaekers, E., Fettweis, M., Vanlierde, E., Vanlede, J., Stassen, P., Elsen, J., Środoń, J., Vandenberghe, N., 2018. Quantitative clay mineralogy as provenance indicator for recent muds in the southern North Sea. Mar. Geol. 398, 48–58. https://doi.org/10.1016/j.margeo.2017.12.011.

An, Y., Liu, J., Zhang, J., Chen, B., Chen, L., Zhang, X., Sheng, C., 2020. Comparative researches on provenance indicators of Huaihe River, Yangtze River and Yellow River sediments. Quaternary Sciences 40, 837–850. https://doi.org/10.11928/j.issn.1001-7410.2020.03.20 in Chinese with English abstract.

Austermann, G., Kling, M., Ifrim, C., Emondt, P.D., Hildenbrand, A., 2021. Quantifying the diagenetic impact in the late Ediacaran and early Palaeozoic of the Avalon Peninsula using illite "crystallinity". Can. J. Earth Sci. 58, 1187–1208. https://doi.org/10.1139/cjes-2020-0207.

Bao, H., Lee, T.-Y., Huang, J.-C., Feng, X., Dai, M., Kao, S.-J., 2015. Importance of Oceanian small mountainous rivers (SMRs) in global land-to-ocean output of lignin and modern biospheric carbon. Sci. Rep. 5, 16217. https://doi.org/10.1038/srep16217.

Bi, L., Yang, S., Li, C., Guo, Y., Wang, Q., Liu, J.T., Yin, P., 2015. Geochemistry of river-borne clays entering the East China Sea indicates two contrasting types of weathering and sediment transport processes. Geochem. Geophys. Geosyst. 16, 3034–3052. https://doi.org/10.1002/2015gc005867.

Bianchi, T.S., Allison, M.A., 2009. Large-river delta-front estuaries as natural "recorders" of global environmental change. PNAS 106, 8085–8092. https://doi.org/10.1073/pnas.0812878106.

Biscaye, P.E., 1965. Mineralogy and sedimentation of recent deep-sea clay in the Atlantic Ocean and adjacent seas and oceans. Geol. Soc. Am. Bull. 76, 803–832. https://doi.org/10.1130/0016-7606(1965)76[803:MASORD]2.0.CO;2.

Brantley, S.L., Shaughnessy, A., Lebedeva, M.I., Balashov, V.N., 2023. How temperature-dependent silicate weathering acts as Earth's geological thermostat. Science 379, 382–389. https://doi.org/10.1126/science.add2922.
Cao, L., Liu, J., Shi, X., He, W., Chen, Z., 2019. Source-to-sink processes of fluvial sediments in the northern South China Sea: Constraints from river sediments in the coastal region of South China. J. Asian Earth Sci. 185, 104020. https://doi.org/10.1016/j.jseaes.2019.104020.
Chen, Y., Chen, N., Li, Y., Hong, H., 2018. Multi-timescale sediment responses across a human impacted river-estuary system. J. Hydrol. 2018 (560), 160–172. https://doi.org/10.1016/j.jhydrol.2018.02.075.
Chen, B., Wang, K., Dong, X., Lin, H., 2021. Long-term changes in red tide outbreaks in Xiamen Bay in China from 1986 to 2017. Estuarine Coastal Shelf Sci. 249, 107095. https://doi.org/10.1016/j.ecss.2020.107095.
Chen, Y., Zhu, G., Lin, X., Wu, F., 2023. The changes of nitrogen and phosphorus contents and their occurrence forms in surface water as affected by flood tide and ebb tide in the tidal reach of the Minjiang River. Acta Scientiae Circumstantiae 1–10 in Chinese with English abstract.
Committee, F.P.L.C.C., 2001. Annals of Fujian Province. Local Chronicles Publishing House, Beijing, China.
Coynel, A., Etcheber, H., Abril, G., Maneux, E., Dumas, J., Hurtrez, J.-E., 2005. Contribution of small mountainous rivers to particulate organic carbon input in the Bay of Biscay. Biogeochemistry 74, 151–171. https://doi.org/10.1007/s10533-004-3362-1.
Cui, G., Liu, Z., Xu, W., Gao, Y., Yang, S., Grossart, H.-P., Li, M., Luo, Z., 2022. Metagenomic exploration of antibiotic resistance genes and their hosts in aquaculture waters of the semi-closed Dongshan Bay (China). Sci. Total Environ. 838, 155784. https://doi.org/10.1016/j.scitotenv.2022.155784.
Dai, S.B., Yang, S.L., Li, M., 2009. The sharp decrease in suspended sediment supply from China's rivers to the sea: Anthropogenic and natural causes. Hydrol. Sci. J. 54, 135–146. https://doi.org/10.1623/hysj.54.1.135.
Deconinck, J.-F., Hesselbo, S.P., Pellenard, P., 2019. Climatic and sea-level control of Jurassic (Pliensbachian) clay mineral sedimentation in the Cardigan Bay Basin, Llanbedr (Mochras Farm) borehole, Wales. Sedimentology 66, 2769–2783. https://doi.org/10.1111/sed.12610.
Deng, K., Yang, S., Bi, L., Chang, Y.-P., Su, N., Frings, P., Xie, X., 2019. Small dynamic mountainous rivers in Taiwan exhibit large sedimentary geochemical and provenance heterogeneity over multi-spatial scales. Earth Planet. Sci. Lett. 505, 96–109. https://doi.org/10.1016/j.epsl.2018.10.012.
Deng, K., Yang, S., Guo, Y., 2022. A global temperature control of silicate weathering intensity. Nat. Commun. 13, 1781. https://doi.org/10.1038/s41467-022-29415-0.
Dill, H.G., 2017. Residual clay deposits on basement rocks: The impact of climate and the geological setting on supergene argillitization in the Bohemian Massif (Central Europe) and across the globe. Earth Sci. Rev. 165, 1–58. https://doi.org/10.1016/j.earscirev.2016.12.004.
Duanmu, Y., 2006. Discussion on several technical problems in the regulation project of Tongshanxi River estuary in Fuding City. Water Science and Technology 4, 31–32 in Chinese.
Ehrmann, W., Schmiedl, G., Hamann, Y., Kuhnt, T., Hemleben, C., Siebel, W., 2007. Clay minerals in late glacial and Holocene sediments of the northern and southern Aegean Sea. Palaeogeogr. Palaeoclimatol. Palaeoecol. 249, 36–57. https://doi.org/10.1016/j.palaeo.2007.01.004.
Esquevin, J., 1969. Influence de la composition chimique des illites sur leur cristallinité. Bull. Centre Rech. Pau-SNPA 3, 147–153.
Evrard, O., Navratil, O., Ayrault, S., Ahmadi, M., Némery, J., Legout, C., Lefèvre, I., Poirel, A., Bonté, P., Esteves, M., 2011. Combining suspended sediment monitoring and fingerprinting to determine the spatial origin of fine sediment in a mountainous river catchment. Earth Surf. Proc. Land. 36, 1072–1089. https://doi.org/10.1002/esp.2133.
Fagel, N., Hillaire-Marcel, C., De Vernal, A., 2007. Chapter Four Clay Minerals, Deep Circulation and Climate. In: Developments in Marine Geology. Elsevier, Amsterdam, pp. 139–184.
Farnsworth, K.L., Milliman, J.D., 2003. Effects of climatic and anthropogenic change on small mountainous rivers: the Salinas River example. Global Planet. Change 39, 53–64. https://doi.org/10.1016/s0921-8181(03)00017-1.
Fujian Province Water Management Institute, 2021a. Fujian Province Soil and Water Conservation Bulletin. Fujian Prov. Water Resour. Bur, Fujian, China.
Fujian Province Water Management Institute, 2021b. Fujian Province Water Resources Bulletin. Fujian Prov. Water Resour. Bur, Fujian, China.
Fujian Province Water Management Institute. http://slt.fujian.gov.cn/ (accessed 13th May 2024).
Galán, E., 2006. Genesis of clay minerals. Dev. Clay Sci. 1, 1129–1162. https://doi.org/10.1016/S1572-4352(05)01042-1.
Gao, J.H., Shi, Y., Sheng, H., Kettner, A.J., Yang, Y., Jia, J.J., Wang, Y.P., Li, J., Chen, Y., Zou, X., Gao, S., 2019. Rapid response of the Changjiang (Yangtze) River and East China Sea source-to-sink conveying system to human induced catchment perturbations. Mar. Geol. 414, 1–17. https://doi.org/10.1016/j.margeo.2019.05.003.
Gao, Y., Yang, Z., Peng, R., Sun, Z., Gao, P., Song, C., 2024. Trade-off impact of carbon-peak target of forest volume and economic development goals on land use/land cover in Fujian. Journal of Beijing Normal University (natural Science) 60, 129–137 in Chinese with English abstract.
Garzanti, E., He, J., Barbarano, M., Resentini, A., Li, C., Yang, L., Yang, S., Wang, H., 2021. Provenance versus weathering control on sediment composition in tropical monsoonal climate (South China) - 2. Sand petrology and heavy minerals. Chem. Geol., 564, 119997. Doi: 10.1016/j.chemgeo.2020.119997.
Gingele, F.X., Deckker, P.D., Hillenbrand, C.-D., 2001. Clay mineral distribution in surface sediments between Indonesia and NW Australia -— source and transport by ocean currents. Mar. Geol. 179, 135–146. https://doi.org/10.1016/S0025-3227(01)00194-3.
Guangdong Province Water Management Institute, 2021. Guangdong Province Water Resources Bulletin. Guangdong Prov. Water Resour. Bur, Guangdong, China.
Guo, Y., 2014. Elemental Geochemistry of the Fluvial Sediments in Zhejiang and Fujian Provinces: Controls of Provenance and Chemical Weathering. Tongji University, Shanghai. M.Sc. thesis (in Chinese with English abstract).
He, J., Garzanti, E., Dinis, P., Yang, S., Wang, H., 2020. Provenance versus weathering control on sediment composition in tropical monsoonal climate (South China)-1. Geochemistry and Clay Mineralogy. Chem. Geol. 558, 119860. https://doi.org/10.1016/j.chemgeo.2020.119860.
He, M., Zheng, H., Huang, X., Jia, J., Li, L., 2013. Yangtze River sediments from source to sink traced with clay mineralogy. J. Asian Earth Sci. 69, 60–69. https://doi.org/10.1016/j.jseaes.2012.10.001.
Hu, B., Li, J., Cui, R., Wei, H., Zhao, J., Li, G., Fang, X., Ding, X., Zou, L., Bai, F., 2014. Clay mineralogy of the riverine sediments of Hainan Island, South China Sea: Implications for weathering and provenance. J. Asian Earth Sci. 96, 84–92. https://doi.org/10.1016/j.jseaes.2014.08.036.
Ito, A., Wagai, R., 2017. Global distribution of clay-size minerals on land surface for biogeochemical and climatological studies. Sci. Data 4, 170103. https://doi.org/10.1038/sdata.2017.103.
Jian, X., Zhang, W., Liang, H., Guan, P., Fu, L., 2019. Mineralogy, petrography and geochemistry of an early Eocene weathering profile on basement granodiorite of Qaidam basin, northern Tibet: Tectonic and paleoclimatic implications. Catena 172, 54–64. https://doi.org/10.1016/j.catena.2018.07.029.
Jian, X., Yang, S., Hong, D., Liang, H., Zhang, S., Fu, H., Zhang, W., 2020a. Seasonal geochemical heterogeneity of sediments from a subtropical mountainous river in SE China. Mar. Geol. 422, 106120. https://doi.org/10.1016/j.margeo.2020.106120.
Jian, X., Zhang, W., Yang, S., Kao, S.-J., 2020b. Climate-Dependent Sediment Composition and Transport of Mountainous Rivers in Tectonically Stable, Subtropical East Asia. Geophys. Res. Lett. 47, e2019GL086150. https://doi.org/10.1029/2019GL086150.
Kao, S.J., Milliman, J.D., 2008. Water and Sediment Discharge from Small Mountainous Rivers, Taiwan: The Roles of Lithology, Episodic Events, and Human Activities. J. Geol. 116, 431–448. https://doi.org/10.1086/590921.
Khan, M.H.R., Liu, J., Liu, S., Seddique, A.A., Cao, L., Rahman, A., 2019. Clay mineral compositions in surface sediments of the Ganges-Brahmaputra-Meghna river system of Bengal Basin, Bangladesh. Mar. Geol. 412, 27–36. https://doi.org/10.1016/j.margeo.2019.03.007.
Kim, S.-W., Choi, E.-K., Kim, J.-W., Kim, T.-H., Lee, K.-H., 2017. Chemical weathering index of clastic sedimentary rocks in Korea. The Journal of Engineering Geology 27, 67–79. https://doi.org/10.9720/kseg.2017.1.67.
Li, T., Cai, G., Wang, C., Liang, K., Ma, S., Luo, W., 2021b. Quantifying clay mineral sources in marine sediments by using end-member mixing analysis. Geo-Mar. Lett. 41, 6. https://doi.org/10.1007/s00367-020-00674-4.
Li, Y., Huang, X., Hiep, N.T., Lian, E., Yang, S., 2021c. Disentangle the sediment mixing from geochemical proxies and detrital zircon geochronology. Mar. Geol. 440, 106572. https://doi.org/10.1016/j.margeo.2021.106572.
Li, Y., Huang, X., Lian, E., Li, C., Xu, J., Yin, P., Song, Z., Yang, S., 2023. Geochemical and provenance heterogeneity of small mountainous river systems in Southeast China. Global Planet. Change 230, 104271. https://doi.org/10.1016/j.gloplacha.2023.104271.
Li, C., Shi, X., Kao, S., Chen, M., Liu, Y., Fang, X., Lü, H., Zou, J., Liu, S., Qiao, S., 2012. Clay mineral composition and their sources for the fluvial sediments of Taiwanese rivers. Chin. Sci. Bull. 57, 673–681. https://doi.org/10.1007/s11434-011-4824-1.
Li, T., Sun, G., Yang, C., Liang, K., Ma, S., Huang, L., Luo, W., 2019. Source apportionment and source-to-sink transport of major and trace elements in coastal sediments: Combining positive matrix factorization and sediment trend analysis. Sci. Total Environ. 651, 344–356. https://doi.org/10.1016/j.scitotenv.2018.09.198.
Li, G., Xia, X., Jia, J., Wang, Y., Cai, T., Gao, S., 2021a. Predicting sediment flux from continental shelf islands, southeastern China. J. Ocean. Limnol. 39, 472–482. https://doi.org/10.1007/s00343-020-9333-0.
Li, D., Xu, Y., Li, Y., Wang, J., Yin, X., Ye, X., Wang, A., Wang, L., 2018. Sedimentary records of human activity and natural environmental evolution in sensitive ecosystems: A case study of a coral nature reserve in Dongshan Bay and a mangrove forest nature reserve in Zhangjiang River estuary, Southeast China. Org. Geochem. 121, 22–35. https://doi.org/10.1016/j.orggeochem.2018.02.011.
Lin, H., 2014. Tidal characteristics in the Sansha Bay of Fujian. Journal of Fujian Fisheries 36, 306–314 in Chinese with English abstract.
Liu, X., Chen, Z., Si, Y., Qian, P., Wu, H., Cui, L., Zhang, D., 2021. A review of tidal current energy resource assessment in China. Renewable Sustainable Energy Rev. 145, 111012. https://doi.org/10.1016/j.rser.2021.111012.
Liu, Z., Colin, C., Huang, W., Chen, Z., Trentesaux, A., Chen, J., 2007a. Clay minerals in surface sediments of the Pearl River drainage basin and their contribution to the South China Sea. Chin. Sci. Bull. 52, 1101–1111. https://doi.org/10.1007/s11434-007-0161-9.
Liu, Z., Colin, C., Huang, W., Le, K.P., Tong, S., Chen, Z., Trentesaux, A., 2007b. Climatic and tectonic controls on weathering in south China and Indochina Peninsula: Clay mineralogical and geochemical investigations from the Pearl, Red, and Mekong drainage basins. Geochem. Geophys. Geosyst. 8, Q05005. https://doi.org/10.1029/2006GC001490.
Liu, Z., Tuo, S., Colin, C., Liu, J.T., Huang, C.-Y., Selvaraj, K., Chen, C.-T.-A., Zhao, Y., Siringan, F.P., Boulay, S., Chen, Z., 2008. Detrital fine-grained sediment contribution from Taiwan to the northern South China Sea and its relation to regional ocean

circulation. Mar. Geol. 255, 149–155. https://doi.org/10.1016/j.margeo.2008.08.003.
Liu, Z., Colin, C., Li, X., Zhao, Y., Tuo, S., Chen, Z., Siringan, F.P., Liu, J.T., Huang, C.-Y., You, C.-F., Huang, K.-F., 2010. Clay mineral distribution in surface sediments of the northeastern South China Sea and surrounding fluvial drainage basins: Source and transport. Mar. Geol. 277, 48–60. https://doi.org/10.1016/j.margeo.2010.08.010.
Liu, H.-C., You, C.-F., Chung, C.-H., Huang, K.-F., Liu, Z.-F., 2011. Source variability of sediments in the Shihmen Reservoir, Northern Taiwan: Sr isotopic evidence. J. Asian Earth Sci. 41, 297–306. https://doi.org/10.1016/j.jseaes.2011.02.013.
Liu, Z., Zhao, Y., Colin, C., Siringan, F.P., Wu, Q., 2009. Chemical weathering in Luzon, Philippines from clay mineralogy and major-element geochemistry of river sediments. Appl. Geochem. 24, 2195–2205. https://doi.org/10.1016/j.apgeochem.2009.09.025.
Liu, Z., Zhao, Y., Colin, C., Stattegger, K., Wiesner, M.G., Huh, C.-A., Zhang, Y., Li, X., Sompongchaiyakul, P., You, C.-F., Huang, C.-Y., Liu, J.T., Siringan, F.P., Le, K.P., Sathiamurthy, E., Hantoro, W.S., Liu, J., Tuo, S., Zhao, S., Zhou, S., He, Z., Wang, Y., Bunsomboonsakul, S., Li, Y., 2016. Source-to-sink transport processes of fluvial sediments in the South China Sea. Earth Sci. Rev. 153, 238–273. https://doi.org/10.1016/j.earscirev.2015.08.005.
Lyons, W.B., Nezat, C.A., Carey, A.E., Hicks, D.M., 2002. Organic carbon fluxes to the ocean from high-standing islands. Geology 30, 443–446. https://doi.org/10.1130/0091-7613(2002)030<0443:OCFTTO>2.0.CO;2.
Lyu, H., Lu, H., 2024. Precipitation is the main control on the global distribution of soil clay minerals. Earth Sci. Rev. 257, 104891. https://doi.org/10.1016/j.earscirev.2024.104891.
Maher, K., 2010. The dependence of chemical weathering rates on fluid residence time. Earth Planet. Sci. Lett. 294, 101–110. https://doi.org/10.1016/j.epsl.2010.03.010.
Maher, K., Chamberlain, C.P., 2014. Hydrologic Regulation of Chemical Weathering and the Geologic Carbon Cycle. Science 343, 1502–1504. https://doi.org/10.1126/science.1250770.
Mei, H., Jian, X., Zhang, W., Fu, H., Zhang, S., 2021. Behavioral differences between weathering and pedogenesis in a subtropical humid granitic terrain: Implications for chemical weathering intensity evaluation. CATENA 203, 105368. https://doi.org/10.1016/j.catena.2021.105368.
Meunier, A., Velde, B., 2004. Illite. Springer-Verlag, Berlin, Origins, Evolution and Metamorphism.
Milliman, J.D., Farnsworth, K.L., 2013. River discharge to the coastal ocean: a global synthesis. Cambridge University Press, Cambridge.
Milliman, J.D., Lee, T.Y., Huang, J.C., Kao, S.J., 2017. Impact of catastrophic events on small mountainous rivers: Temporal and spatial variations in suspended- and dissolved-solid fluxes along the Choshui River, central western Taiwan, during typhoon Mindulle, July 2–6, 2004. Geochim. Cosmochim. Acta 205, 272–294. https://doi.org/10.1016/j.gca.2017.02.015.
Milliman, J.D., Syvitski, J.P.M., 1992. Geomorphic/Tectonic Control of Sediment Discharge to the Ocean: The Importance of Small Mountainous Rivers. J. Geol. 100, 525–544. https://doi.org/10.1086/629606.
Nayak, K., Garzanti, E., Lin, A.-T.-S., Castelltort, S., 2022. Taiwan river muds from source to sink: Provenance control, inherited weathering, and offshore dispersal pathways. Sed. Geol. 438, 106199. https://doi.org/10.1016/j.sedgeo.2022.106199.
Nesbitt, H.W., Fedo, C.M., Young, G.M., 1997. Quartz and feldspar stability, steady and non-steady-state weathering, and petrogenesis of siliciclastic sands and muds. J. Geol. 105, 173–191. https://doi.org/10.1086/515908.
Pang, H., Pan, B., Garzanti, E., Gao, H., Zhao, X., Chen, D., 2018. Mineralogy and geochemistry of modern Yellow River sediments: Implications for weathering and provenance. Chem. Geol. 488, 76–86. https://doi.org/10.1016/j.chemgeo.2018.04.010.
Peng, S., 2020. 1-km monthly precipitation dataset for China (1901–2021). National Tibetan Plateau/third Pole Environment Data Center. https://doi.org/10.5281/zenodo.3185722.
Peng, S., 2019. 1-km monthly mean temperature dataset for China (1901-2021). National Tibetan Plateau/Third Pole Environment Data Center. Doi: 10.11888/Meteoro.tpdc.270961. https://cstr.cn/18406.11.Meteoro.tpdc.270961.[dataset].
Ranasinghe, R., Wu, C.S., Conallin, J., Duong, T.M., Anthony, E.J., 2019. Disentangling the relative impacts of climate change and human activities on fluvial sediment supply to the coast by the world's large rivers: Pearl River Basin. China. Sci. Rep. 9, 9236. https://doi.org/10.1038/s41598-019-45442-2.
Ren, X., Nie, J., Saylor, J.E., Wang, X., Liu, F., Horton, B.K., 2020. Temperature Control on Silicate Weathering Intensity and Evolution of the Neogene East Asian Summer Monsoon. Geophys. Res. Lett., 47, e2020GL088808. https://doi.org/Doi: 10.1029/2020GL088808.
Romans, B.W., Castelltort, S., Covault, J.A., Fildani, A., Walsh, J.P., 2016. Environmental signal propagation in sedimentary systems across timescales. Earth Sci. Rev. 153, 7–29. https://doi.org/10.1016/j.earscirev.2015.07.012.
Shantou water resources information network. https://www.shantou.gov.cn/stwater/ (accessed 23th November 2023).
Shen, X., Jian, X., Li, C., Liu, J.T., Chang, Y.-P., Zhang, S., Mei, H., Fu, H., Zhang, W., 2021. Submarine topography-related spatial variability of the southern Taiwan Strait sands (East Asia). Mar. Geol. 436, 106495. https://doi.org/10.1016/j.margeo.2021.106495.
Su, N., Yang, S., Guo, Y., Yue, W., Wang, X., Yin, P., Huang, X., 2017. Revisit of rare earth element fractionation during chemical weathering and river sediment transport. Geochem. Geophys. Geosyst. 18, 935–955. https://doi.org/10.1002/2016gc006659.
Sun, S., Zhu, L., Hu, K., Li, Y., Nie, Y., 2022. Quantitatively distinguishing the factors driving sediment flux variations in the Daling River Basin, North China. CATENA 212, 106094. https://doi.org/10.1016/j.catena.2022.106094.
Syvitski, J.P.M., 2003. Supply and flux of sediment along hydrological pathways: research for the 21st century. Global Planet. Change 39, 1–11. https://doi.org/10.1016/S0921-8181(03)00008-0.
Tabor, N.J., Myers, T.S., 2015. Paleosols as indicators of paleoenvironment and paleoclimate. Annu. Rev. Earth Planet. Sci. 43, 333–361. https://doi.org/10.1146/annurev-earth-060614-105355.
Vanacker, V., Ameijeiras-Mariño, Y., Schoonejans, J., Cornélis, J.-T., Minella, J.P.G., Lamouline, F., Vermeire, M.-L., Campforts, B., Robinet, J., Van de Broek, M., Delmelle, P., Opfergelt, S., 2019. Land use impacts on soil erosion and rejuvenation in Southern Brazil. CATENA 178, 256–266. https://doi.org/10.1016/j.catena.2019.03.024.
Vörösmarty, C.J., Meybeck, M., Fekete, B., Sharma, K., Green, P., Syvitski, J.P., 2003. Anthropogenic sediment retention: major global impact from registered river impoundments. Global Planet. Change 39, 169–190. https://doi.org/10.1016/S0921-8181(03)00023-7.
Wan, K., Bao, X., Yao, Z., Wan, X., Xia, Y., 2014. Tidal and residual current characteristic at mouth of shachenggang channel. OCEANOLOGIA ET LIMNOLOGIA SINICA, 45, 669–675 (in Chinese with English abstract). Doi: 10.11693/hyhz20130315002.
Wang, L., 2024. Feasibility Evaluation of Clay Minerals as Indicators of Chemical Weathering and Climate Change. Xiamen University, Xiamen (in Chinese with English abstract) M.Sc. thesis.
Wang, Y., Fan, D., Liu, J.T., Chang, Y., 2016. Clay-mineral compositions of sediments in the Gaoping River-Sea system: Implications for weathering, sedimentary routing and carbon cycling. Chem. Geol. 447, 11–26. https://doi.org/10.1016/j.chemgeo.2016.10.024.
Wang, L., Jian, X., Fu, H., Zhang, W., Shang, F., Fu, L., 2023. Decoupled local climate and chemical weathering intensity of fine-grained siliciclastic sediments from a paleo-megalake: An example from the Qaidam basin, northern Tibetan Plateau. Sediment. Geol. 454, 106462. https://doi.org/10.1016/j.sedgeo.2023.106462.
Wang, S., Rao, W., Qian, J., He, M., Mao, C., Li, K., Feng, Y., Zhao, J., 2021. Clay Mineralogy of Surface Sediments in the Three Gorges Reservoir: Implications for Sediment Provenances and Weathering Regimes. Clay Clay Mineral. 69, 52–67. https://doi.org/10.1007/s42860-020-00106-5.
Wang, C., Sun, Q., Jiang, S., Wang, J.-K., 2011. Evaluation of pollution source of the bays in Fujian province. Procedia Environ. Sci. 10, 685–690. https://doi.org/10.1016/j.proenv.2011.09.110.
Wang, H., Yang, Z., Saito, Y., Liu, J.P., Sun, X., Wang, Y., 2007. Stepwise decreases of the Huanghe (Yellow River) sediment load (1950–2005): Impacts of climate change and human activities. Global Planet. Change 57, 331–354. https://doi.org/10.1016/j.gloplacha.2007.01.003.
Wang, A.-J., Ye, X., Lin, Z.-K., Wang, L., Lin, J., 2020. Response of sedimentation processes in the Minjiang River subaqueous delta to anthropogenic activities in the river basin. Estuar. Coast. Shelf. Sci. 232, 106484. https://doi.org/10.1016/j.ecss.2019.106484.
Warr, L.N., 2022. Earth's clay mineral inventory and its climate interaction: A quantitative assessment. Earth Sci. Rev. 234, 104198. https://doi.org/10.1016/j.earscirev.2022.104198.
Warr, L.N., Cox, S.C., 2016. Correlating illite (Kübler) and chlorite (Árkai) "crystallinity" indices with metamorphic mineral zones of the South Island. New Zealand. Appl. Clay Sci. 134, 164–174. https://doi.org/10.1016/j.clay.2016.06.024.
Warr, L.N., Ferreiro Mählmann, R., 2015. Recommendations for Kübler Index standardization. Clay Mineral. 50, 283–286. https://doi.org/10.1180/claymin.2015.050.3.02.
Wheatcroft, R.A., Goñi, M.A., Hatten, J.A., Pasternack, G.B., Warrick, J.A., 2010. The role of effective discharge in the ocean delivery of particulate organic carbon by small, mountainous river systems. Limnol. Oceanogr. 55, 161–171. https://doi.org/10.4319/lo.2010.55.1.0161.
Wu, K., Liu, S., Shi, X., Colin, C., Bassinot, F., Lou, Z., Zhang, H., Zhu, A., Fang, X., Rahim Mohamed, C.A., 2022. The effect of size distribution on the geochemistry and mineralogy of tropical river sediments and its implications regarding chemical weathering and fractionation of alkali elements. Lithosphere 2022, 8425818. https://doi.org/10.2113/2022/8425818.
Xi, Y., Shi, Y., Dai, X., Liu, Z., Wu, Z., 2016. Spatial difference and provenance of clay minerals as tracers of intertidal sediments in Hangzhou Bay. Acta Sedimentologica Sinica 34, 315–325 in Chinese with English abstract.
Xu, K., Milliman, J.D., Li, A., Paul Liu, J., Kao, S.-J., Wan, S., 2009. Yangtze- and Taiwan-derived sediments on the inner shelf of East China Sea. Cont. Shelf Res., 29, 2240–2256. https://doi.org/Doi: 10.1016/j.csr.2009.08.017.
Yang, X., 1995. Clay minerals of suspended sediments in Oujiang River. Marine Science Bulletin 14, 86–92 in Chinese with English abstract.
Yang, S., Yin, P., 2018. Sediment source-to-sink processes of small mountainous rivers under the impacts of natural environmental changes and human activities. Marine Geology & Quaternary Geology 38, 1–10 in Chinese with English abstract.
Youn, J., Yang, S., Park, Y.A., 2007. Clay minerals and geochemistry of the bottom sediments in the northwestern East China Sea. Chin. J. Ocean. Limnol. 25, 235–246. https://doi.org/10.1007/s00343-007-0235-1.
Yu, Z., Colin, C., Bassinot, F., Wan, S., Bayon, G., 2020. Climate-driven weathering shifts between highlands and floodplains. Geochem. Geophys. Geosyst. 21, e2020GC008936. https://doi.org/10.1029/2020GC008936.
Yue, Y., Zheng, Z., Huang, K., Chevalier, M., Chase, B.M., Carré, M., Ledru, M.-P., Cheddadi, R., 2012. A continuous record of vegetation and climate change over the past 50,000years in the Fujian Province of eastern subtropical China. Palaeogeogr. Palaeoclimatol. Palaeoecol. 365–366, 115–123. https://doi.org/10.1016/j.palaeo.2012.09.018.

Zhang, C., Hu, G., Yu, R., Liu, Y., 2015. Speciation and bioavailability of heavy metals in sediments from tidal reach of the Jinjiang River. Environmental Chemistry 34, 505–513 in Chinese with English abstract.

Zhang, Y., Huang, G., Wang, W., Chen, L., Lin, G., 2012. Interactions between mangroves and exotic Spartina in an anthropogenically disturbed estuary in southern China. Ecology 93, 588–597. https://doi.org/10.1890/11-1302.1.

Zhang, S., Jian, X., Liu, J.T., Wang, P., Chang, Y.P., Zhang, W., 2022. Climate-driven drainage reorganization of small mountainous rivers in Taiwan (East Asia) since the last glaciation: The Zhuoshui River example. Palaeogeogr. Palaeoclimatol. Palaeoecol. 586, 110759. https://doi.org/10.1016/j.palaeo.2021.110759.

Zhao, T., Xu, S., Hao, F., 2023. Differential adsorption of clay minerals: Implications for organic matter enrichment. Earth Sci. Rev. 246. https://doi.org/10.1016/j.earscirev.2023.104598.

Zhao, Y., Zou, X., Gao, J., Wang, C., Li, Y., Yao, Y., Zhao, W., Xu, M., 2018. Clay mineralogy and source-to-sink transport processes of Changjiang River sediments in the estuarine and inner shelf areas of the East China Sea. J. Asian Earth Sci. 152, 91–102. https://doi.org/10.1016/j.jseaes.2017.11.038.

Zhu, J., 2001. A preliminary analysis on the influencing factors of low tide variation in Nangang reach of Jiulongjiang River. Hydrology 21, 32–35 in Chinese.